MODELLING, SIMULATION AND OPTIMISATION OF A CRUSHING PLANT

by

BLESSING NDHLALA

Submitted in accordance with the requirements for the degree of

MAGISTER OF TECHNOLOGIAE: ENGINEERING: ELECTRICAL

at the

UNIVERSITY OF SOUTH AFRICA

Supervisor: Prof. FRANCOIS MULENGA

July 2017

ABSTRACT

African copper PLC's flagship is the copper producing Mowana mine located 129 km from Francistown in the North-Eastern part of the Republic of Botswana. The processing operation at Mowana is a standard flotation plant designed to produce copper concentrates from oxide, supergene, and sulphide ores. The expected average output of 16.2 tons per hour of copper concentrates has never been attained since plant commissioning. The major bottleneck has been established to be located around the crushing circuit of the Mowana production chain.

The major hypotheses of this research are that performance in a crushing plant is adversely influenced by moderate and discrete changes in the process. The ultimate objective is to develop a dynamic process simulator, administered in Simulink/MATLAB® background, for application in the design of a control model utilising two crusher variables and a self-tuning control algorithm.

In this research work, a process model describing the dynamic operation of an Osborn 57S gyrasphere cone crusher is investigated. Modelling of the Mowana crushing circuit is carried out by combining the steady-state and dynamic components of the crushing equipment in the Simulink/Matlab® environment. Eccentric speed (*ES*) and closed-side setting (*CSS*) are amongst the important inputs to the models. The rest of the inputs (crusher power, crusher cavity level, federate, pulley diameters, liner wear measurement, number of teeth of the pinion and bevel gear) are extracted from the data collected across the Mowana mine crushing circuit. While it has been demonstrated that the crusher *CSS* is the most influential controllable parameter, it has also been demonstrated that crusher capacity and power can be used effectively to optimise the circuit. The use of crushing power and cavity level control is suitable for the

crushing circuit since the crushers are running on a constant ES and the CSS is set and reset manually.

The outcome of the study presents an insight into the optimization of the Mowana mine crushing circuit through the design of a self-tuning controller for the cone crusher and for prototyping, parameters of a PID controller were determined in the Simulink/MATLAB® environment. The simulation involved the optimisation of the control model as a function of the cavity level of and the power drawn by the cone crusher. A self-tuning control algorithm at PLC and SCADA level of control was then tested. This formed the simulations and training platform.

The outcome of the simulations carried out in this research needs to be validated against the real Mowana crushing process control upgrade. This will then inform the modifications and recommended crusher motor resizing exercise to be implemented.

DEDICATION

This study is dedicated to my parents, Obadiah and Gracewin, my siblings, Ossie, Sharo, Thandie and Nono, my wife Bertha, my son Nigel and my beautiful daughters, Amanda and Natania, for their endless love and support.

ACKNOWLEGEMENTS

First and foremost I would like to thank my God for his spiritual guidance through this project.

It gives me much pleasure to extend my sincere and heartfelt gratitude and appreciation to all those who, in their various ways, have made this study a reality. First and foremost, my study supervisor, Dr Francois Mulenga, for his guidance, enlightenment, inspiration and encouragement received during this research project. Engineer Albert Bhila, Auto Control, for all those sleepless nights of endless PLC and SCADA simulations. Engineer Tawanda Samuriwo, the head of section at Mowana Mine, for his support and willingness to grant me the required leave and use of company facilities and equipment. My thanks are due to the Manager Metallurgy, Elijah Mugiya, Senior Laboratory Chemist, Kyle Karihindi , Timothy Maker for all the IT support and the Mowana mine team I cannot mention by name, for their support during the execution of certain project works. Not leaving out those engineers, Lecturers and colleagues to whom, through their experience, written works and discussions, I am greatly indebted.

The University of South Africa for accepting me to study at this institution and the continuous unwavering encouragement received throughout the years.

DECLARATION

I hereby declare that this dissertation submitted for a Magister Technologiae : Engineering : Electrical at the University of South Africa degree, is my own original work and has not been submitted to any other institution of higher learning. I also declare that all sources cited or quoted are indicated and acknowledged by means of a comprehensive list of references. I understand that any violation of the above will be cause for disciplinary action by the Institution and can evoke penal action from the sources which have thus not been properly cited or from whom proper permission has not been taken when needed.

_____
(Signature)

BLESSING NDHLALA

(Name of the student)

46683933

(Student Number)

Date: _____

DEFINITION OF TERMS

The following definitions and terms have been used in this research:

Choke feeding	A feeding regime to the crusher that keeps the crusher's cavity full at all time
Closed Circuit	A crushing process arrangement in which part of the material produced by the crusher is circulated back to the same crusher for further crushing
Comminution	Generic name referring to any minerals processing operation used to achieve size reduction of minerals and ores
Crushing plant	An arrangement of equipment which reduces or changes the size of large rocks into a specified smaller size
Crushing Ratio	Ratio between in-coming feed and out-going product. It is normally measured of the 80% size point, i.e. the size at which 80 % of the material passes through the screen aperture. It is given by$Crushing\ Ratio = \frac{Feed_{80}}{Product_{80}}$
Dynamic Simulation	The use of a computer program to model the time varying behaviour of a system
Flakiness Index	Metrics describing the shape of a rock particle
Grading	Determination of the crushed product's particle size distribution
Liner	The inner part of tools to be used for crushing
Mantle	Crushing liner fastened to the moving eccentric main shaft
Optimisation	Finding an alternative with the most cost effective or the highest achievable performance under given constraints
Power draw	The electrical energy supplied to operate an

	electrical machine
Reduction Ratio	The ratio of the crusher feed size to the crusher product size
Screening	Method used in separating different sized particles
Segregation	Movement of smaller particles tending to separate them from the mixture with larger particles
Software development	The collective procedure involving computer programming, documenting, testing, and debugging involved in building and supporting applications and frameworks resulting in a software product.

ABBREVIATION

ANFIS	**Adaptive-Network-based Fuzzy Inference System**
BD	**Bulk Density**
CAP	**Crusher Capacity [t/h]**
CAV	**Cavity Geometry**
CDF	**Cumulative Distributive Function**
CSS	**Closed Side Setting, minimum distance between liner and concave at the discharge end of cavity**
DDF	**Differential Distributive Function**
Feq	**Feed grading equivalent size, [mm]**
FFI	**Feed material Flakiness Index**
FG	**Feed grading, also known as particle size distribution of feed material, [mm]**
FI	**Flakiness Index**
FIFO	**First in – First out**
LA	**Crushability**
LIFO	**Last in – First out**
M	**Moisture or water content of rock material, [%]**
Nstr	**Nominal Stroke length of the crusher, [mm]**
OSS	**Open Side Setting, maximum distance between liner and concave at the discharge end of cavity**
PID	**Proportional Integral Derivative**
PLC	**Programmable Logic Controller**
Q	**Feed rate or material mass flow, [t/h]**
RMSE	**Root Mean Square Error**
SCADA	**Supervisory Control and Data Acquisition**
SG	**Specific gravity or absolute weight of the rock material per unit volume, [t/m^3]**

SYMBOLS

K	Steady-state gain
J	Exponent indicating the presence of integration
CZ	Number of crushing zones
ES	Crusher eccentric speed, [rpm]
T_d	Material residence time in crusher cavity, [s]
eSTR1	Effective stroke length of the last crushing zone, [mm]
Y	Model output
X	Vector of inputs
B	Vector of the fitted constant
nSTR	Nominal Stroke of the crusher
MINnSTR	Minimum nominal Stroke of the Crusher
m_{tank}	Material mass in the tank, [t]
Q_{in_tank}	Mass flow into the tank, [t/h]
Q_{out_tank}	Mass flow out of the tank, [t/h]
$E_{Rittinger}$	Energy input
$C_{Rittinger}$	Material constant
P_{80}	The particle size corresponding to 80 % of the product passing
f_{80}	The particle size corresponding to 80 % of the feed passing.
E_H	The specific breakage energy (According to Hukki)
K_H	Hukki's constant
$f(z)$	The probability of fragmentation of grains of size z
φ	The vertical angle of mantle at closed-side setting
K	The steady-state gain

$\boldsymbol{\lambda}$	The transport delay
$\boldsymbol{T_1}$	The dominant time constant
$\boldsymbol{T_2}$	The non-dominant time constant
$\boldsymbol{j}$	The exponent indicating the presence of integration
$\boldsymbol{S}$	The diagonal matrix representing the specific breakage of particles of size i
$\boldsymbol{B}$	The lower diagonal matrix, where B_{ij} represents the fraction of particles of size fraction j appearing in the fraction size i after breakage

TABLE OF CONTENTS

LIST OF FIGURES

LIST OF TABLES

CHAPTER 1 INTRODUCTION

1.1 BACKGROUND

Crushing circuits form a vital and integral function of the mining, mineral processing and metallurgical industry. The continuous demand for high quality crushed product and the subsequent high downstream costs associated with end-products highlights the need for effective crusher control (Andrew *et al*., 2000). However, the implementation of any control strategy comes with a great challenge due to the harsh environment crushing plants operate in.

Crushing is known to be an energy intensive process. Hofler (1980) argued that crushing represents approximately 3 – 5 % of all electricity consumed on a national level. It is therefore of paramount importance that the power drawn and energy consumed by a crusher be accurately modelled for simulation, optimisation and control purposes.

The energy consumption of a crusher can be influenced by factors such as feed rate, feed size distribution, ore hardness, crusher operating settings and volume of ore in the crusher cavity. All these factors can be integrated into a framework that enables a phenomenological description of the crushing process. King (2001) provides a comprehensive review of the underlying models applicable to mineral processing in general and crushing in particular. With the aid of computers a range of options can be simulated, optimum operating conditions as well as circuit designs determined with relative ease and accuracy. This offers then answers to plant design and optimisation under specific conditions (Gupta and Yan, 2006).

In terms of the development of a successful control strategy, a good understanding of the process dynamics and equipment characteristics, a

broad knowledge of control principles and a well-designed schema are amongst the most important factors that need to be considered.

The accurate design and operation of a crushing circuit are of paramount importance. These are guided by the search for minimal power consumption for maximal throughput and product size meeting the downstream requirements. The successful implementation of such a constrained optimization problem results in considerable organisational and economic gain. It is therefore clear that without disrupting production, simulation can be utilised as a useful tool in investigating the response and performance of a crushing circuit while determining the optimum operating conditions.

The purpose of this work is to design a process control system for a crusher. To this end, dynamic models for crushing process (i.e. particle size reduction) are developed for optimisation and simulation. The crushing models are then used in the design of a process control system for the crushing circuit. The test work and simulation are conducted at the Mowana mine in order to provide invaluable data for calibration and validation purposes. The approach taken can therefore be split into four main stages: test work, modelling, simulation, and optimisation. The word ‘simulation’ here refers to the designing and testing of the process control system using an appropriate specialised software package.

1.2 PRESENTATION OF THE RESEARCH PROJECT

African copper PLC’s flagship is the copper producing Mowana mine located 129 km from Francistown in the North-Eastern part of the Republic of Botswana. The processing operation at Mowana is a standard flotation plant designed to produce copper concentrates from oxide, supergene, and sulphide ores.

Since the commissioning of the plant in 2008, a lot of operating and control changes have been implemented to increase the plant throughput

and reduce operating costs. Of special mention were the replacement of the secondary and tertiary cone crushers as well as the vibrating screens, the installation of the LAROX PF1011 filter press and the tuning of control loops within the flotation area. Despite these changes, the desired plant throughput has still not been consistently acquired as shown in Figures 1.1 and 1.2.

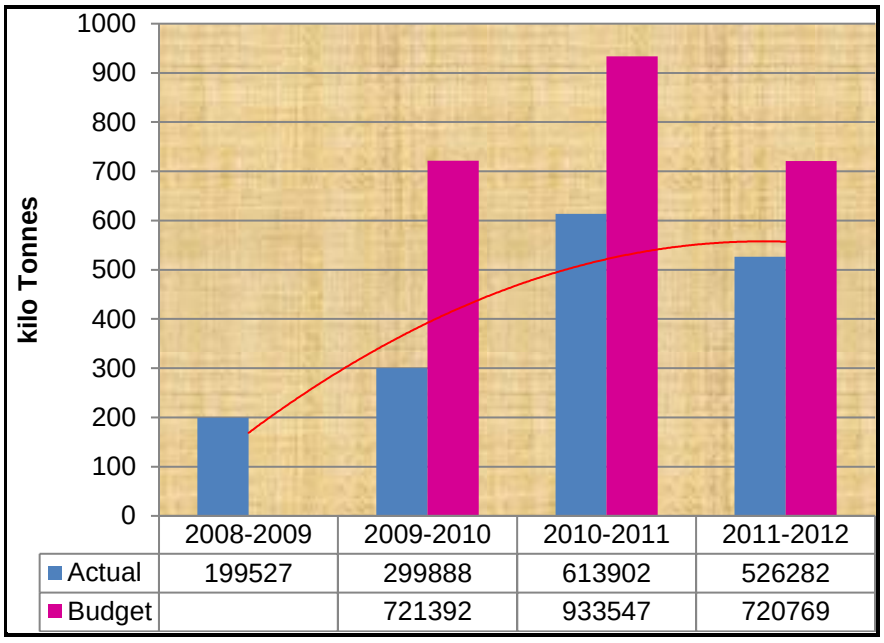

Figure 1.1 Primary crusher tonnage: 2008 through to 2012

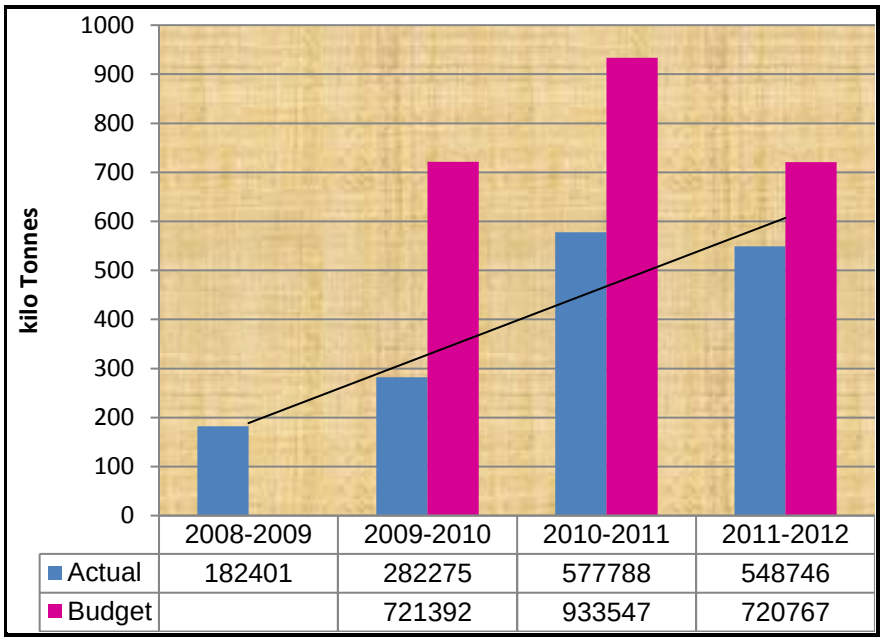

Figure 1.2 Secondary and tertiary crusher tonnage: 2008 through 2012

The major bottleneck has been established to be located around the crushing circuit of the Mowana production chain.

The implemented changes have brought the following inherent challenges:

- Premature failure of equipment possibly from usage beyond specifications;
- Introduction of additional equipment yielded high maintenance costs and increased pressure on production and engineering personnel due to increase in equipment;
- Unwanted plant stoppages at the crusher circuit for closed-side setting (*CSS*) adjustments; hence, increase in downtime and running costs
- Premature liner wear of liners due to metal to metal interaction inside the crusher;
- Low plant design throughput.

It is believed that poor performance is attributed mainly to the fact that past optimisation was equipment-centred and was overlooking the equipment arrangement. Understanding and describing the process behaviour would be a better approach.

In this study, optimisation is solved through simulations. Simulink®, software in Matlab®, is used to design a control model for the Mowana crushing plant. The purpose of the control is to reduce overloading and stoppage of the crusher to a minimum. The solution is expected to integrate two crusher variables and a self-tuning algorithm at PLC and SCADA level.

1.3 RESEARCH AIM AND OBJECTIVES

The purpose of this research is to formulate ways and means for optimising the operation of the Mowana crushing plant.

The ultimate objective is to develop dynamic process models and control software for the crushing circuit consisting of secondary and tertiary cone crushers, vibrating screens, and belt conveyors. The dynamic model is built using the Simulink® platform under the Matlab® software.

The research strategy can be summarised as follows:

- Development of models, software and hardware that enables the optimisation of the Mowana crushing circuit
- Selection of suitable sensors for the closed loop control circuits
- Proposal of a virtual Process Plant as a tool for control verification but also as a training simulator
- Design of an optimal control model

The main hypothesis of this research is that performance in a crushing plant is adversely influenced by moderate and discrete changes in the process. In order to curb the effects of these changes, a dynamic simulator has to be developed. In addition to this, the research concentrates on the plant operation and performance of a crushing plant under dry conditions, i.e. with no water present.

In order to achieve the objectives assigned, two key research questions are posed to guide the work:

1. Can the implementation of closed-loop control systems in the process yield and improve production?

2. Besides the commonly used parameter, i.e. closed-side setting *CSS*, in the adjustment of the product in cone crushers, is it possible to use other parameters for circuit optimisation?

The successful answers to the two research questions can hopefully lead to reduction in unit operating costs while resulting in increased throughput as well as improved product size and downstream performance (Napier-Munn *et al.*, 1999).

1.4 DELIMITATION OF THE WORK

The scope of this research has been set in terms of the complexity of the control system to be designed. A generic simulation model, consisting of eight individual models, is used in the design of the control system for the cone crusher circuit. Among the eight individual models, the flow model is used to provide crusher specific input parameters.

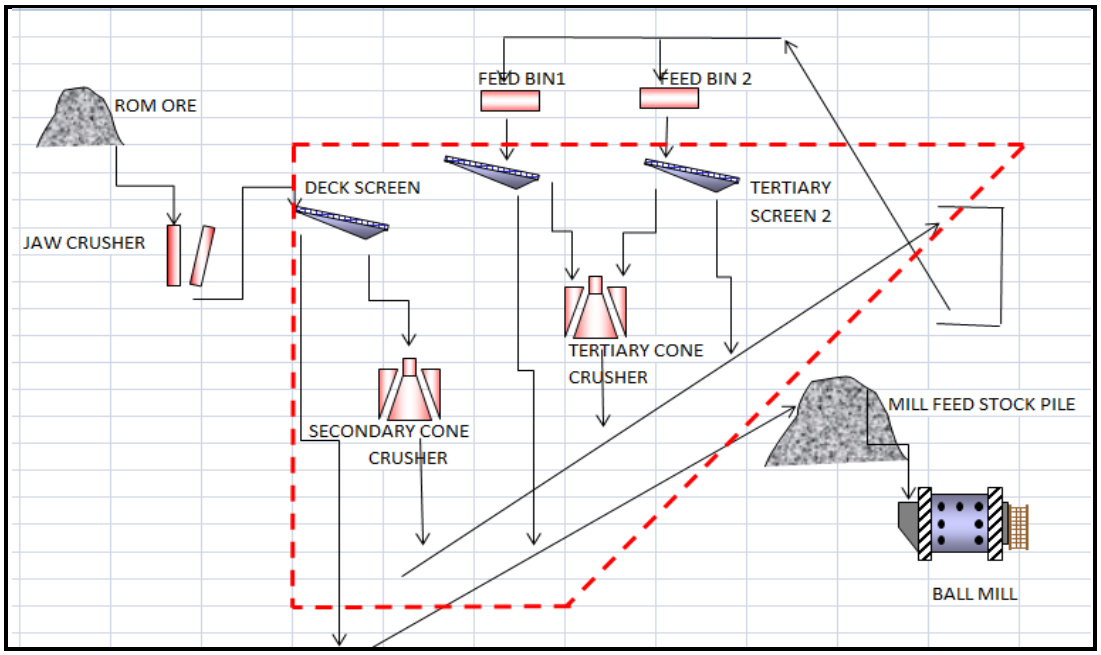

Figure 1.3 Overview of the Mowana crushing plant with the area of focus depicted in the dashed box

Figure 1.3 depicts the area of study for the Mowana processing plant. Focus is on the secondary and tertiary crushers of the crushing circuit. The upstream operations, i.e. coarse ore stock piling, drilling, blasting, primary jaw crushing, are beyond the scope of this research. Similarly, downstream processes which include fine ore stockpiling, milling and flotation are also outside the scope set out.

For the above, it is evident that the definition of the final product should be done in reference to the material leaving the last stage of crushing. Furthermore, the properties of the rock material such as ore grade, rock flakiness, amongst others, are not taken into consideration in the development of the models underpinning this work.

The hypotheses of this research are that performance in a crushing plant is adversely affected by gradual and discrete changes in the process and that more efficient crushing plants can be attained by first optimizing a given crushing process through simulations before designing the actual crushing circuit. The conducted research can therefore be split into three main stages, namely modelling, simulation and optimization.

However, the research attempts to describe the Mowana crushing circuit by blending the steady-state and dynamic components of the crushing equipment in the Simulink/Matlab® environment and models depicting the dynamics of actuators and disturbances. The presented model is used in investigating the fundamental disturbances from the process control standpoint while ascertaining the controllability of the crushing circuit with the help of the Simulink/MATLAB® environment.

1.5 RESEARCH APPROACH

The selection of resolution methods for a problem is anchored on the nature of the problem in question. This means that the focus is on the problem rather than on the method resolving the problem. The problem-

based approach illustrated in Figure 1.4 has been exploited in this research project (Evertsson, 2000; Lee, 2012).

The methodology suggests that the initial step is to identify the nature of the problem through observations such as literature reviews, data acquisition and guiding experiments. On identification, the character of the problem decides the selection of the method to be implemented. The selection is based on the performed observations as to which method would be best capable to resolve the problem in question. This is an iterative process which will repeat itself pending a method resolved to be the suitable is established. The acquired model is then verified by simulations and experiments validating the results obtained from the model in question.

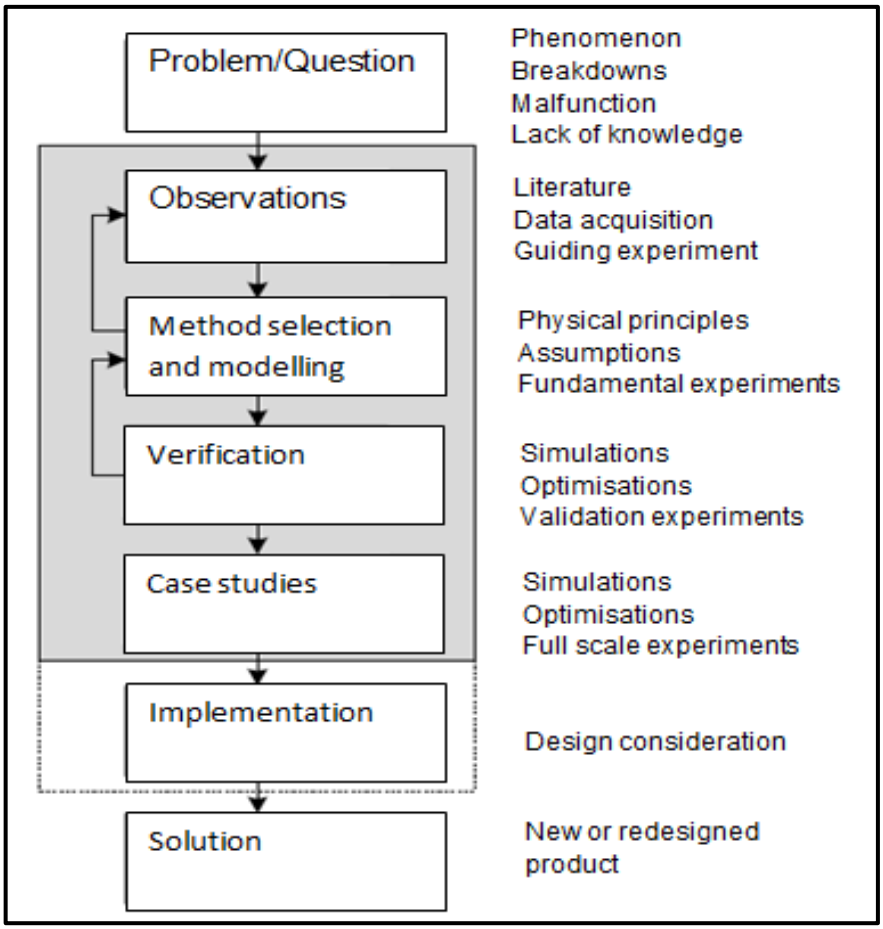

Figure 1.4 Applied problem-oriented research model (Evertsson, 2000)

Subsequent to the verification of the model and validation of the obtained results a case study is conducted, in communion with the Mowana Mine crushing circuit. Simulation, optimisation and full scale experiments are then executed in order to draw conclusions pertaining the effects and potential improvements to be implemented. According to Evertsson (2000), the newly acquired knowledge will then be formulated in the design considerations, which will be implemented through the improvements of the original crushing circuit or through a complete circuit redesign.

1.6 LAYOUT OF THE DISSERTATION

The dissertation is divided into seven chapters.

Chapter 1 gives a general introduction to this research and presents its aims and objectives. Research questions are formulated and delimitations of the research undertaken are clarified.

Chapter 2 introduces the classical comminution theories. Research that has focused on the dynamic simulation of crushing plants is also presented. Areas of research that have studied factors influencing the crushing plant performance are reviewed.

Chapter 3 presents the applied research model and introduces the research methodology used. The chapter also covers the experimental plans of this research. Methods of material characterization, sample preparation and size analysis are discussed in detail. Test procedures for both laboratory and computer simulations are outlined. Chapter 4, on the other hand, discusses the results. A great deal is devoted to the phenomenological modelling of the crushing circuit under investigation.

Chapter 5 describes the optimization algorithm and motivates the choice of the optimization method. Finally, Chapter 6 summarises the important

findings of the research and answers the research questions stated in Chapter 1.

CHAPTER 2 LITERATURE REVIEW

Until the dawn of the last decade, research carried out on the modelling, simulation and optimisation of crushing plants has been limited. The main focus has been on discrete production units with little attention paid to their interaction, the plant operation, control and instrumentation.

In this chapter, progress made on the dynamic simulation of crushing circuits and factors influencing plant efficiency is reviewed. The aim is to provide an overview to the research on crushing circuits relevant to the present research.

2.1 COMMINUTION THEORY

Over the years theories for the determination of the energy required in rock size reduction have been put forward. Rittinger (1867), Kick (1885), and Bond (1952) presented empirical energy-size reduction equations. These are well known as the three classical comminution theories and their general formulation was presented by Walker *et al*. (1937).

Rittinger (1867) postulated that the surface area produced by comminution is directly proportional to the energy consumed

$$E_{Rittinger} = C_{Rittinger}\left[\frac{1}{P_{80}} - \frac{1}{f_{80}}\right] \quad (2.1)$$

where $E_{Rittinger}$ is the energy input

$C_{Rittinger}$ is a material constant

P_{80} is the particle size corresponding to 80 % of the product passing

f_{80} is the particle size corresponding to 80 % of the feed passing.

The second theory came from Kick (1885). It states that the work required for breakage is proportional to the reduction in volume of the particles concerned.

$$E_{Kick} = -C_{Kick}\left[\frac{P_{80}}{f_{80}}\right] \quad (2.2)$$

Bond (1952) came up with a more useful formula which posited that the total energy E_{Bond} specific to any size is inversely proportional to the square root of the particle size:

$$E_{Bond} = C_{Bond}\left[\frac{1}{\sqrt{P_{80}}} - \frac{1}{\sqrt{f_{80}}}\right] = W_I\left[\frac{10}{\sqrt{P_{80}}} - \frac{10}{\sqrt{f_{80}}}\right] \quad (2.3)$$

In Equation (2.3), the Bond work index W_I expresses the resistance that the material opposes to crushing or grinding.

Trials have been made to substantiate that the relationships of Rittinger, Kick and Bond are perceptions of one universal equation. Hukki (1975) postulated that the relationship between energy and particle size is a conglomerate model of the three laws. This was presented in the form of the following differential equation:

$$dE_H = -K_H \frac{dZ}{Z^{f(z)}} \quad (2.4)$$

where E_H is specific breakage energy (According to Hukki)

K_H is Hukki's constant

$f(z)$ is the probability of fragmentation of grains of size z

In addition to the assumptions made by the authors of the first three energy-based laws, Equation (2.4) takes into account the probability of fragmentation $f(z)$ of grains according to their original dimensions. This probability is equated to unity for large particles and tends to zero for ultrafine particles.

The outcome of Equation (2.4) is the energy-size relationship shown in Figure 2.1. It can be seen that Kick's theory applies to coarse particles (i.e.

larger than 10 mm). Bond's, on the other hand, applies down to 100 μm whereas Rittinger's applies to sizes smaller than 100 μm. Moreover, the chances of breakage in comminution are more likely for large particles, and rapidly diminish for fine sizes (Willis, 2006).

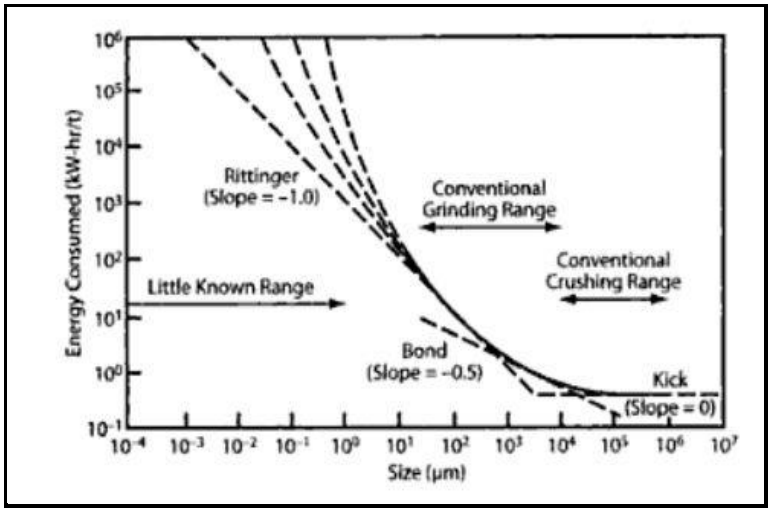

Figure 2.1 Energy used in Comminution (Hukki, 1975)

Perhaps the most important point to make is that the shortcoming of the three comminution theories is that they do not take account of particle interaction and energy consumed by plastic deformation (Juhasz and Opoczky, 1990).

2.2 MODELLING OF THE CRUSHING PLANT

Since the 19th century, the quest for models able to predict crusher performance has proven to be a challenge. The fundamental problem has been a difficulty in characterising complex heterogeneous rock materials. However, models developed since then can be categorised into four dominant groups: fundamental models, classical models, black-box models, and empirical models. The last two are reviewed in this section because of their wide use and better predicting abilities (Napier-Munn *et al*., 1996).

2.2.1 Black-box models

In 1877 Charles Brown invented Gyratory crushers which around 1881 were developed by Gates and were then named Gates crusher (Truscott, 1923). The cone crusher is considered to be the miniature portrayal of a Gyratory crusher (Gupta and Yan, 2006). Figure 2.2 shows the basic operating principle of a cone crusher (Evertsson, 2000).

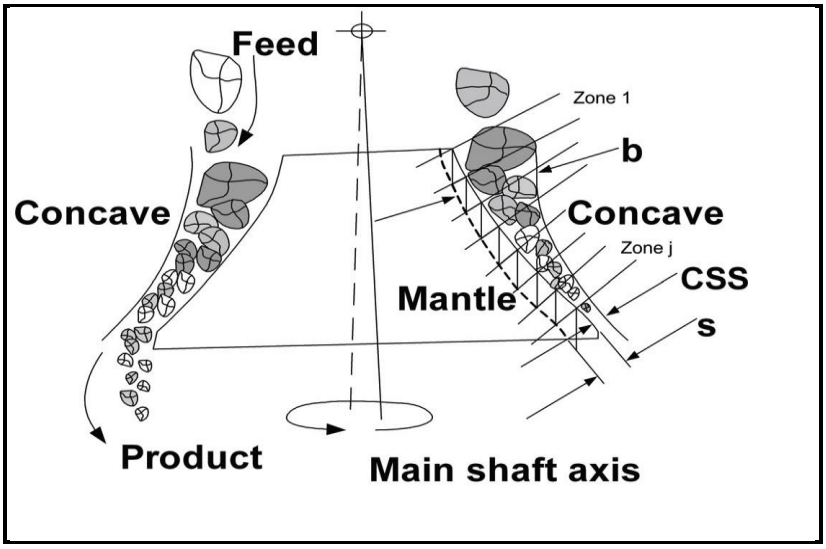

Figure 2.2 Schematic illustration of a cone crusher (Evertsson, 2000)

The feed material is exposed to repetitive compressive actions inside the crushing cavity as it is comminuted between movable liner (mantle) and fixed liner (concave). The concave chamber is attached to the crusher frame and the mantle to the eccentrically moving main shaft (Itävuo, 2009). The eccentric shaft is nutating around the centre of eccentricity at a fixed distance from the geometric centre point with a constant speed. The rotating cone can be simplified as a bar linkage mechanism (Eloranta, 1995). Evertsson (2000) characterised the crushing process in a cone crusher by dividing the crushing chamber into diverse crushing zones. This means that the crushing process is discretised, where each crushing zone corresponds to a crushing event performed by a compression that is defined by the ratio of the stroke **s** and the bed height **b** (refer to Figure 2.2).

The Whiten model is the most generic in the black-box class of models. Indeed, Whiten (1972) assumed that particles entering the crushing chamber could either be broken or dropped through the crusher unbroken. Then, the broken particles can further be crushed or discharged past the crusher. Thus, the crusher can be regarded as consisting of two zones: a single breakage zone and a classification zone in which particles are selected for exit or for re-breakage. Figure 2.3 illustrates symbolically the zones of this cone crusher model and the internal flows between them.

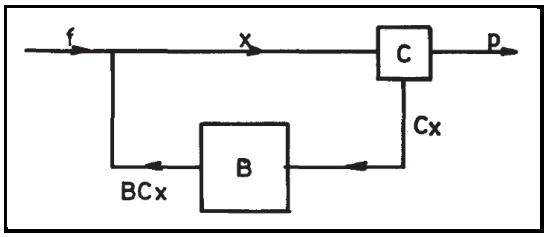

Figure 2.3 Breakage events in a crusher (after Whiten, 1972)

A mass balance at the first node of Figure 2.3 yields: $f + Bcx = x$. Similarly, at the second node: $x = Cx + p$. By combining these two equations, Equation (2.5), known as the 'Whiten model' of a crusher, can be produced:

$$p = [I - C][I - CB]^{-1} f \qquad (2.5)$$

In Equation (2.5), p and f are the products and feed flow rates; I is the unit matrix; B is the breaking matrix in which the diagonal matrix gives the proportion of particles entering the breakage region; C is the classification function, i.e. a diagonal matrix giving the proportion of particles in each size grouping which enters the breakage zone.

The model, also known as the Selection-Breakage model, suffers the drawback that it requires the knowledge of the crusher geometry and feed input data.

2.2.2 Empirical models

Empirical models have been attained by employing regression techniques while striving to correlate machine variables and crusher performance. An illustration is provided by Karra (1982) who related machine variables, throughput and power consumption:

$$Throughput = 1.663(sin\varphi)1.224(throw)0.773(CSS)0.507 \quad (2.6)$$

$$Power\ consumption = 19.547(throughput)0.849(P_{80}) - 0.984 \quad (2.7)$$

where P_{80} is the 80 % passing size of the product

φ is the vertical angle of mantle at closed-side setting

$throw$ is the stroke of the mantle while rotating and nutating around the eccentric shaft. It is labeled $nSTR$ in Figure 2.4.

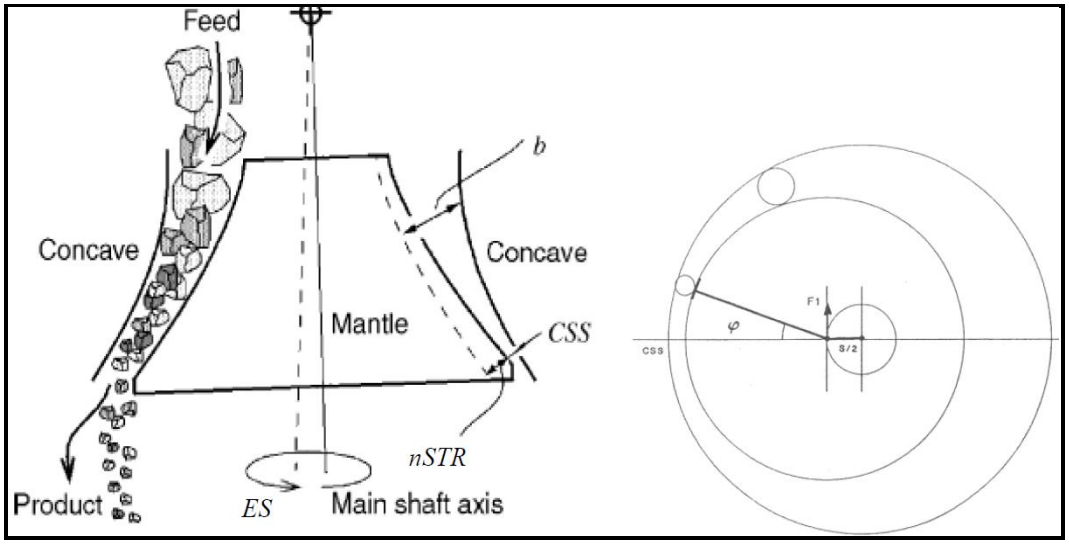

Figure 2.4 A cone crusher with the machine variables (after Itävuo, 2009)
ES is the rotational speed of the eccentric or mantle

Empirical approaches are renowned as quick solutions for industrial challenges and can deliver guides for operational purposes. But they are only pertinent to a specific category of crushers and installations. However, they cannot be adopted as generic models.

2.3 DYNAMICS MODELLING

Balchen and Mumme (1988) were able to demonstrate that linear dynamics such as crushers can be modelled using the First Order Plus Dead Time (FOPDT) model and the Second Order Plus Dead Time (SOPDT). FOPDT models are used as a starting point for dynamics modelling since they generally give satisfactory results of the process dynamics in most industrial applications (Balchen, 1988).

If the step response of a system behaves like a second order model then the use of SOPDT should be considered. However, so many industrial plants are modelled by a FOPTD transfer function (Giuseppe, 2009). By that as it may, the two standard process models are given below:

$$G_1(s) = \frac{K}{s^j(1+T_1 s)} e^{-\lambda s} \tag{2.8}$$

$$G_2(s) = \frac{K}{s^j(1+T_1 s)+(1+T_2 s)} e^{-\lambda s} \tag{2.9}$$

where K is the steady-state gain

λ is the transport delay

T_1 is the dominant time constant

T_2 is the non-dominant time constant

j is the exponent indicating the presence of integration, usually j = 0

Note that Equation 2.8 represents the mathematical form of a process model of first order whereas Equation 2.9 is that of second order.

2.4 SIMULATION OF A FULL CRUSHING PLANT

Simulation could be applied as a suitable instrument for investigating the operation and performance of crushing plant circuits. They make the evaluation of various scenarios and the identification of optimum operating conditions easy. Different software packages have been developed and a number have been commercialised with varying degrees of success. This has not deterred the development of simulators for mineral processing units, especially in the last decade. Typical steady-state software

packages are JKSimMet (JKTech, 1989), SIMBAL (CANMET, 1989), USIM PAC (Broussand *et al*., 1988) and MODSIM (King, 2001).

Steady-state simulation packages have been widely used for crushing plant optimisations (Khosrow, 2001; Luis and Bahena, 2001; Renner and LaRosa, 2005), but are limited to ideal situations. Indeed, any process is subject to change in performance and efficiency with time; steady-state simulators do not cater for this.

Dynamic models, on the other hand, evaluate each time-dependent variable. Hence the simulation of transient conditions is achievable (Sbarbaro, 2010). That is why the demand for the implementation of dynamic simulations in plant optimisation has been on the rise worldwide.

One of the most widely used platforms for dynamic modelling is the Simulink® environment of the Matlab® software.

Itävuo (2009) successfully created a dynamic process model for a single crushing stage plant implemented in the Matlab/Simulink® environment. The model is a combination of neuro-fuzzy ANFIS networks, steady-state regression, actuators and disturbances. ANFIS is a form of artificial neural network developed upon Tagadi-Sugeno fuzzy inference framework. The simulation period was considerably long, but the outcome was useful in the development of a control system.

Later, Itävuo *et al*. (2011) presented a dynamic model of a gyratory cone crusher for control system design. Modelling was carried out as a combination of neuro-fuzzy ANFIS networks, log-transformed regression and Laplace transform transfer function models. However, full-scale testing is still needed for validation.

Airikka (2012) came up with a dynamic simulator for a mobile three-stage crushing plant. The simulation model was developed for a real Metso Lokotrack crushing plant having a jaw crusher C120 and two cone crushers; namely, GP300S and GP300C. The simulation method did not

focus on modelling feed material or aggregate size distribution. Size distribution was considered as a non-changing dynamic. This assumption is not realistic as the crushers have different grading with different settings and speeds. Notwithstanding this, the assumption is deemed sufficient for simulating total flow and material levels.

Of special mention amongst the commercial software packages on the market are SysCad, Aspentech, Aspen Plus, MSC Adams and MetProSim. They can also be used for dynamic modelling and have their respective strengths and weaknesses.

2.5 OPTIMISATION OF CRUSHERS

Crusher optimisation has received less consideration in the past. This could be due to the lack of accurate and fast-sensing devices and the known relationship between manipulated variables and required objectives (Atta, 2013). Up till the dawn of the last decade, most crushers were controlled by their closed-side setting (*CSS*). This is ascribed to the fact that the eccentric speed (*ES*) was assumed to have less effect on the crusher capacity and product size distribution (Hulthén, 2010). Following the work by Evertson (1998 and 1999), a clear trend in the effect of the *ES* and the *CSS* on the total throughput and size distribution began to emerge. In line with this, the work by Hulthén and Evertsson (2009) can be regarded as a forerunner in that on-line optimisation in which a finite State Machine for throughput inflation altering the *CSS* was done. Next was a related algorithm adjusting the eccentric speed with promising results (Hulthén and Evertsson, 2008 – 2011).

2.6 FACTORS INFLUENCING CRUSHING PLANT PERFOMANCE

Several factors influence production achievement in a crushing circuit. These factors can be arranged under three categories: ore characteristics, equipment factors, and operation factors (Boyut and Siniflandirma, 2013).

Depending on the abrasiveness of the rock material and the duration of use of the screen clothes, vibrating screen wear with time and hence pass larger sizes of particles (Hulthen, 2010). This is a great challenge to a crushing plant as specified size reduction is crucial to the circuit downstream. A direct consequence of this would be the decrease in both downstream crushing capacity and discharge rate (Boyut and Siniflandirma, 2013).

Crushing circuits just as all other production processes are sensitive to variations which come with time since the process is continuous and equipment is exposed to changes (Itävuo, 2009). Variations brought about by degrading equipment, if not minimised, have adverse effects over the plant capacity as they compromise product quality. Hulthen (2010) observed that production of a crusher is influenced by manganese liner erosion. He then showed that a worn crushing chamber that has experienced bodily changes has a profile different to that of a new chamber. This has a bearing on the capacity of the crusher, the size and shape of the product. By the same token, Lindqvist *et al*. (2006) investigated experimentally the influence of particle size on wear rate. He was able to show that the wear is proportional to particle size and to the square root of the crushing pressure. In contrast, wear on vibrating screens has not received much research attention as yet.

Improper material handling and segregation can have a negative effect on the crushing plant performance and final product quality. A study on segregation in cone crushers was carried out by Quist (2012) using the discrete element method (DEM). However, not much has been done since then.

On a final note, Itävuo (2009) went on to categorise the influences of crushing process variables and known disturbances on crusher operation. He identified three control variables: controllable parameters (*CCS* and *ES*), constant or settable parameters (nSTR and Cavity geometry) and disturbances (moisture, feed grading, crushability, feed rate, specific

gravity, and feed flakiness index). His review of past studies revealed that the effect of each control variable has been considered in some form. However, while one parameter was investigated, the rest were assumed to be constant. Consequently, the possibility of parameters interaction was ignored with varied insight in the research findings.

2.7 REVIEW SUMMARY

Size reduction is a complex phenomenon. The literature review has brought forth the fact that the three classical comminution theories do not take account of particle interaction and energy consumed by plastic deformation. That is why industrial scale experiments have to be performed to study the properties of the ore and laboratory experiments to characterize the ore from a fundamental point of view.

The experimentation should provide a platform for collecting data relevant to the development of models capable of predicting crusher performance. In this chapter, it has been shown that this can be done following either the steady-state paradigm or the dynamic one. In the first instance, black-box and empirical models are widely use. However, black-box models suffer the drawback that the crusher geometry and the feed input data are required. Likewise, empirical models are limited in their window of applicability.

When considering the dynamic paradigm, crushers can be modelled using the First Order Plus Dead Time (FOPDT) model and the Second Order Plus Dead Time (SOPDT). Each model has its own strengths and can complement the steady-state description of the crusher. Indeed a steady-state model of a crusher by means of the Whiten model (also known as the selection-breakage model) is not always sufficient.

In this research work, a process model describing the dynamic operation of an Osborn 57S gyrasphere cone crusher is investigated. Modelling is carried out by combining the steady-state and dynamic components of the

crushing equipment in the Simulink/Matlab® environment. Eccentric speed (*ES*) and closed-side setting (*CSS*) are amongst the important inputs to the models. They are extracted from the data collected across the Mowana mine crushing circuit. That is what is described in detail in the next chapter.

CHAPTER 3 METHODOLOGY

Industrial scale experiments were conducted on a crushing circuit at Mowana mine. The facility has two Osborn crushers for both secondary and tertiary operations. The secondary crusher, an Osborn 57S gyrasphere cone crusher, was selected for the experiment, the key reason being its open circuit configuration which ensures constant feed properties in every test. An industrial sampling program was initiated to measure the ore properties followed by laboratory procedures for characterization. The tests were completed over a five day period. The objective of the tests was to wholly acquire data relating to the feed and machine settings to be used for simulations and modelling of the Mowana mine crushing circuit.

Sample- to-lab reports were captured and stored on Excel spreadsheets and backed up on every update. The reports were also were also backed up to a separate hard drive. Each data base has a single owner and only that person may enter data and or make changes to the data bases.

3.1 INDUSTRIAL SCALE EXPERIMENTS

Five different runs were performed at a targeted CSS of 16 ± 2mm with belt cuts performed for each run and feed sampled for the first, third and fifth run to prevent segregation and in order to acquire a representative sample of the coarse ore stockpile. The standard practice adopted for the collection of a stockpile sample in this research was the stopped – belt cut sampling method. This came with an objective to capture the same ore size distribution hence avoiding a biased result. Samples are collected from different sampling points on the stockpile by sampling after the second and fourth run.

A test sequence was designed in order to control the experiment. This was for diverse reasons including personal safety, to trivialize the chances of data, and sample loss, quality of samples and time management. Before

the initial test, with the ore feeders running on manual, the crushing circuit was ran until it attained a steady state. This was followed by a dry run to facilitate testing of each step. The tests followed the sequence of steps outlined below:

1) The crusher CSS was set
2) The crusher ES was noted
3) Started feeding the crushing circuit with feeders selected to manual mode
4) Ran until choked condition and steady feed was attained
5) Started the data logging and ran for 30 minutes
6) Stopped data logging
7) Tripped the crusher feed conveyor
8) Performed a lockout on the feed conveyor
9) Carried out a belt cut
10) De isolated the feed conveyor and ran the circuit

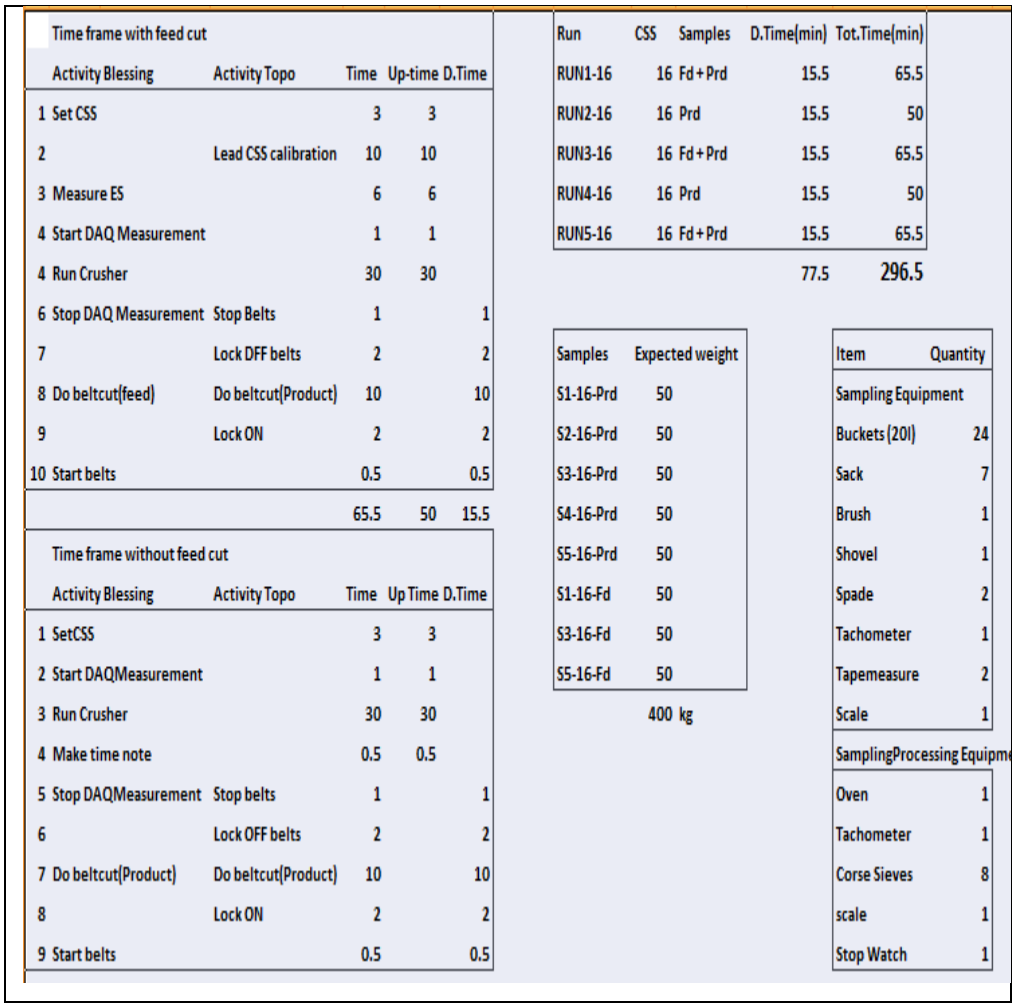

Time frame with feed cut

	Activity Blessing	Activity Topo	Time	Up-time	D.Time
1	Set CSS		3	3	
2		Lead CSS calibration	10	10	
3	Measure ES		6	6	
4	Start DAQ Measurement		1	1	
4	Run Crusher		30	30	
6	Stop DAQ Measurement	Stop Belts	1		1
7		Lock DFF belts	2		2
8	Do beltcut(feed)	Do beltcut(Product)	10		10
9		Lock ON	2		2
10	Start belts		0.5		0.5
			65.5	50	15.5

Time frame without feed cut

	Activity Blessing	Activity Topo	Time	Up Time	D.Time
1	SetCSS		3	3	
2	Start DAQMeasurement		1	1	
3	Run Crusher		30	30	
4	Make time note		0.5	0.5	
5	Stop DAQMeasurement	Stop belts	1		1
6		Lock OFF belts	2		2
7	Do beltcut(Product)	Do beltcut(Product)	10		10
8		Lock ON	2		2
9	Start belts		0.5		0.5

Run	CSS	Samples	D.Time(min)	Tot.Time(min)
RUN1-16	16	Fd+Prd	15.5	65.5
RUN2-16	16	Prd	15.5	50
RUN3-16	16	Fd+Prd	15.5	65.5
RUN4-16	16	Prd	15.5	50
RUN5-16	16	Fd+Prd	15.5	65.5
			77.5	296.5

Samples	Expected weight
S1-16-Prd	50
S2-16-Prd	50
S3-16-Prd	50
S4-16-Prd	50
S5-16-Prd	50
S1-16-Fd	50
S3-16-Fd	50
S5-16-Fd	50
	400 kg

Item	Quantity
Sampling Equipment	
Buckets (20l)	24
Sack	7
Brush	1
Shovel	1
Spade	2
Tachometer	1
Tapemeasure	2
Scale	1
SamplingProcessing Equipme	
Oven	1
Tachometer	1
Corse Sieves	8
scale	1
Stop Watch	1

Figure 3.1 Industrial Scale Experiment Plan

Figure 3.1 illustrates a test plan for the full scale experiments carried out on the Mowana mine secondary crusher.

Due to the sized rock particles, the feed samples were contained in reinforced polymer bags. Each bag was distinctly marked for the sample number and date of experiment.

The samples were analysed in the laboratory for specific gravity, moisture and particle size distribution which according to Itävuo (2009) are the most influential disturbance parameters in the operation of a crusher in an ore processing plant.

3.1.1 Closed side setting Measurement

The procedure involves the turning of a hydraulic motor coupled to the adjusting ring. The thread in the bowel closes and opens the chamber as the bowel moves to the desired position. During the adjustment, the teeth counted by a proximity switch will display the gap opening on a local digital counter.

The following steps were taken to set the CSS of the secondary crusher:

1) Stopped the feed to the crusher and ran the crusher empty
2) Set the crusher to manual control
3) Activated crusher close/open through the respective inch buttons on the control panel
4) Verified the direction of rotation of the crusher head, clockwise for gap closing and the reverse for gap opening
5) Repeated steps 3 and 4 until the required CSS is achieved

For the CSS measurement verification 5 pieces of lead attached to different strings were simultaneously dropped into the crusher for about 5 seconds. This will shape the piece of lead by the closest part of the crushing chamber without passing through the machine. A Vernier caliper was then used to obtain the smallest measure of the parts compressed by the crusher. The average of these five readings was the CSS.

Figure 3.2 CSS Measurement

Figure 3.2 shows a lead piece attached to a string placed in the crusher for CSS measurement and the measurement of the deformed lead using a Vernier caliper.

3.1.2 Liner wear measurement

The liner wear had to be determined to ensure the liner profiles remain a constant in all the performed experiments. The digital counter for CSS measurement is reset immediately after replacing the crusher chamber liners. To determine the amount of liner wear before the commencing of any experiment the following steps were taken:

1) Stopped the crusher. Locked out the power to the crusher drive motor leaving the power to the hydraulic console.
2) In manual mode moved the function control switch to crush
3) Closed the crusher gap till the liners (mantle and Concave ring) made contact with each other. Released the close button as soon as contact was made

The value on the digital counter was observed. If no wear has occurred since the last display reset, the display will read zero. Any negative reading will be an indication of wear. This value was recorded before making a display reset.

3.1.3 Eccentric speed measurement

The initial step was to physically count and note down the teeth of the pinion and bevel gear for the gear ratio determination.

Figure 3.3 Physical count of number of teeth on gears

Figure 3.3 illustrates the bevel gear, on the left hand side, and the pinion gear whose number of teeth were counted for ES calculation.

Repeated measurements, with average readings calculated, of the motor and driven countershaft pulley were performed using a Vernier caliper. With the crusher running empty, the motor pulley speed was measured using a digital tachometer. Figure 3.4 illustrates the measuring points on a crusher driving pulley and gear link schematic layout.

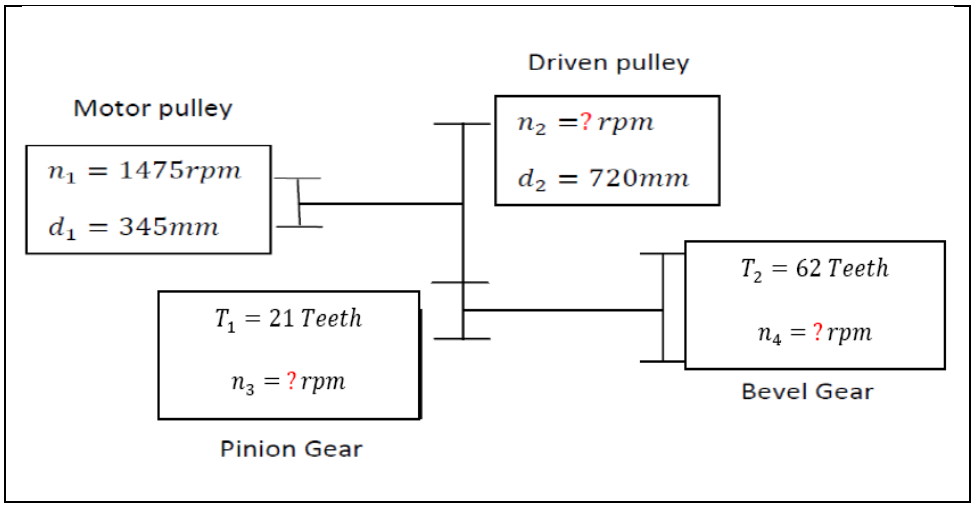

Figure 3.4 Secondary Crusher Site Layout Schematic Diagram

Equation 3.1 was used for the computation of the crusher eccentric speed

$$n_3 \times T_1 = n_4 \times T_2 \quad (3.1)$$

Where n_3 is the pinion gear speed, $T_1$is the pinion gear number of teeth, n_4 is the crusher eccentric speed and $T_2$is the bevel gear number of teeth.

Table 3.1 illustrates the equipment used in this exercise and their specifications

Table 3.1 Equipment used in crusher ES determination

Equipment Used	Specifications
Digital Tachometer	Hellerman Tyton T6236 Accuracy ± 0.05% Sampling time 0.8 seconds
Electric Motor	WEG 260 Kw,1490rpm,525 V,340A
Vernier Calipers	Vernier Accuracy ± 0.05mm

For experimental control purposes the tests followed the following sequence:

1) Took note of the crusher pinion and bevel gear ratio and the motor and pinion pulley mean diameters
2) Ran crusher whilst empty for about a minute to make sure it was under no load.
3) Selected the rpm mode on the tachometer and installed the rpm adaptor on its shaft
4) With the tachometer adaptor pressed lightly against the centre hole of the rotating shaft took note of the reading once the reading stabilised
5) Repeated step 4 five times and used the mean as the pinion speed
6) Used equation 3.1 to compute the *ES*

Figure 3.5 illustrates the motor speed measurements using a tachometer

Figure 3.5 Motor speed measurements using a tachometer

3.2 LABORATORY EXPERIMENTS

For ore characterization all the samples were collected from the belt cuts in clearly marked sample handling bags and sealed buckets, specifying date time and sample number, were stored in the sample preparation room in the laboratory at the Mowana mine for analysis. Figure 3.6 shows the samples which were collected in sealed buckets to avoid moisture losses plastic bags due to the rock sizes.

Figure 3.6 Samples from a belt cut in the Laboratory to be analysed

3.2.1 Moisture Determination

Table 3.2 shows the equipment which was used in the determination of moisture in the samples from the belt cuts

Table 3.2 Equipment used in crusher Moisture determination

Equipment	Description
Drying Oven	Preset at 105˚C ± 0.05
Top pan balance	Metler Toledo SB24001, Max 24100g, e= 1g, Min 5g, d= 1g/.1g
Drying Tray	1050 x 550 x 250)mm

The following steps were formulated to determine the moisture content in the samples.

1) Recorded the weight of the empty tray (W1) on the moisture determination excel spreadsheet
2) Placed a portion of the sample in the drying tray
3) Weighed the tray and the sample on the top pan balance scale and record the weight (W2)
4) Placed the tray into the drying oven
5) Recorded the time the sample was placed in the oven
6) Left the sample in the drying oven for 2-4 hours
7) At the end of the prescribed drying period removed the tray from the oven
8) Cooled the tray in an inert atmosphere for 30 minutes
9) Weighed the tray and record the weight (W3)
10) Emptied the contents of the tray into a labeled sample bag or container
11) Washed and cleaned the tray

Calculated the moisture content for each sample as follows:

$$\%\ Moisture = \frac{Wet\ Weight - Dry\ Weight}{Wet\ Weight} \times 100 \quad (3.2)$$

Or

$$\%\ Moisture = \frac{(W2 - W1) - (W3 - W1)}{(W2 - W1)} \times 100 \quad (3.3)$$

The equations 3.2 and 3.3 were used to calculate the percentage moisture. The data collected during the experiment was entered and backed up on the spreadsheet template illustrated in figure 3.7.

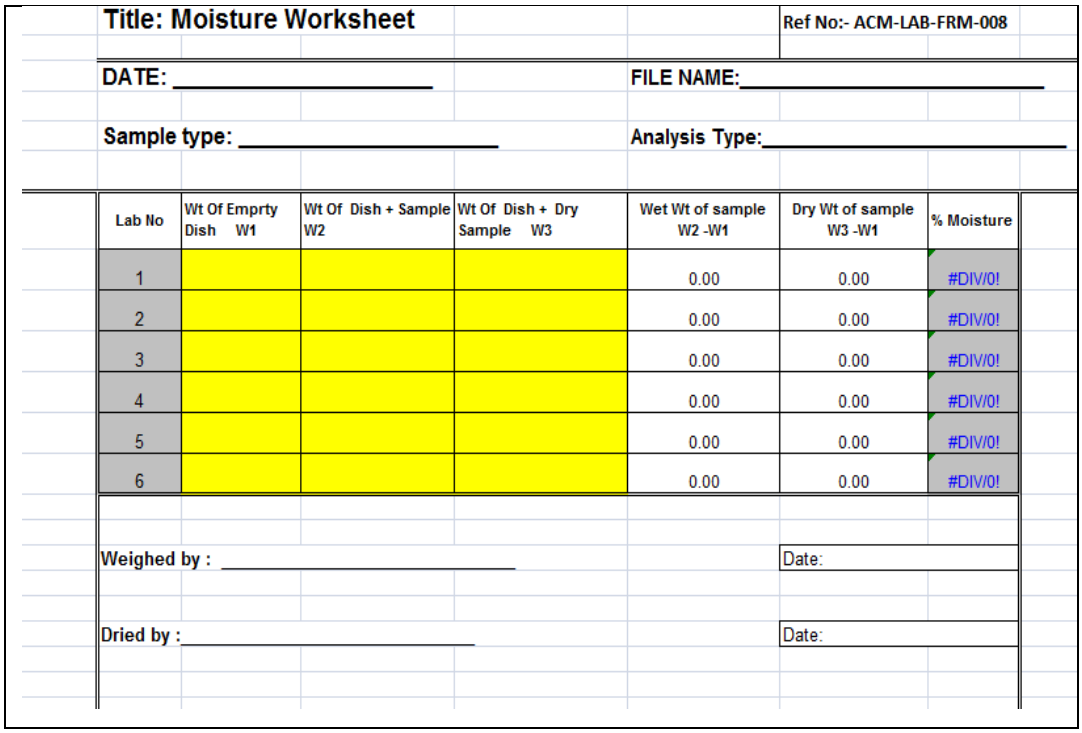

Title: Moisture Worksheet

Ref No:- ACM-LAB-FRM-008

DATE: _____

FILE NAME:_____

Sample type: _____

Analysis Type:_____

Lab No	Wt Of Emprty Dish W1	Wt Of Dish + Sample W2	Wt Of Dish + Dry Sample W3	Wet Wt of sample W2 -W1	Dry Wt of sample W3 -W1	% Moisture
1				0.00	0.00	#DIV/0!
2				0.00	0.00	#DIV/0!
3				0.00	0.00	#DIV/0!
4				0.00	0.00	#DIV/0!
5				0.00	0.00	#DIV/0!
6				0.00	0.00	#DIV/0!

Weighed by : _____ Date:

Dried by :_____ Date:

Figure 3.7 Moisture work sheet image

3.2.2 Particle Size Distribution Analysis

Table 3.3 illustrates the equipment used to carry out the Particle Size Distribution:

Table 3.3 Equipment used in ore PSD determination

Equipment	Description
Sieves	Sieve sizes(mm): 53.0,37.5,26.5,19.0,16.0,11.2,8.0,4.0
Top pan balance	Metler Toledo SB24001, Max 24100g, e= 1g, Min 5g, d= 1g/.1g
Brush	Soft and Wire brushes

For experimental control purposes the tests followed the following sequence:

1) Checked the test sieves for holes in the mesh
2) Checked that the test sieves are clean. If they were not clean blew with compressed air or clean with a stiff brush. Whilst taking care not to perforate the mesh.
3) Stacked the sieves. The coarser screen must be at the top with the finest at the bottom.
4) Placed a portion of the total ore obtained from the belt cut onto the top screen (53mm)
5) Shook the sieve stack for about 10 minutes
6) Brushed any sample which was retained or trapped on the mesh top most sieve before removing it. Also lightly brushed the underside of the mesh.
7) Removed the first sieve and inverted it into a sample bag marked the sieve size and date
8) Repeated steps 6 and 7 for all the sieves whilst brushing and cleaning them
9) Obtained the weight of each fraction retained on each sieve
10) Obtained the weight of the fraction retained in the receiver
11) The total weight of each fraction was to be equal to the mass of the sample taken
12) Any differences were attributed to dust losses
13) Repeated step 2 up to 12 for the remainder of the whole sample

Figure 3.8 Samples being loaded into a sieve stack

Figure 3.8 illustrates the loading of the feed sample into a sieve stack and the range of the sieves making the stack is made of. The weight of the material retained on each sieve is used to calculate the percentage of the sample retained on that sieve as determined by equation 3.4:

$$\%\ Retained\ on\ sieve = \frac{Weight\ of\ Material\ Returned\ on\ sieve}{Total\ weight\ of\ the\ sample\ from\ Belt} \times 100 \quad (3.4)$$

The input weights are entered and backed up in a spreadsheet illustrates in figure 3.9.

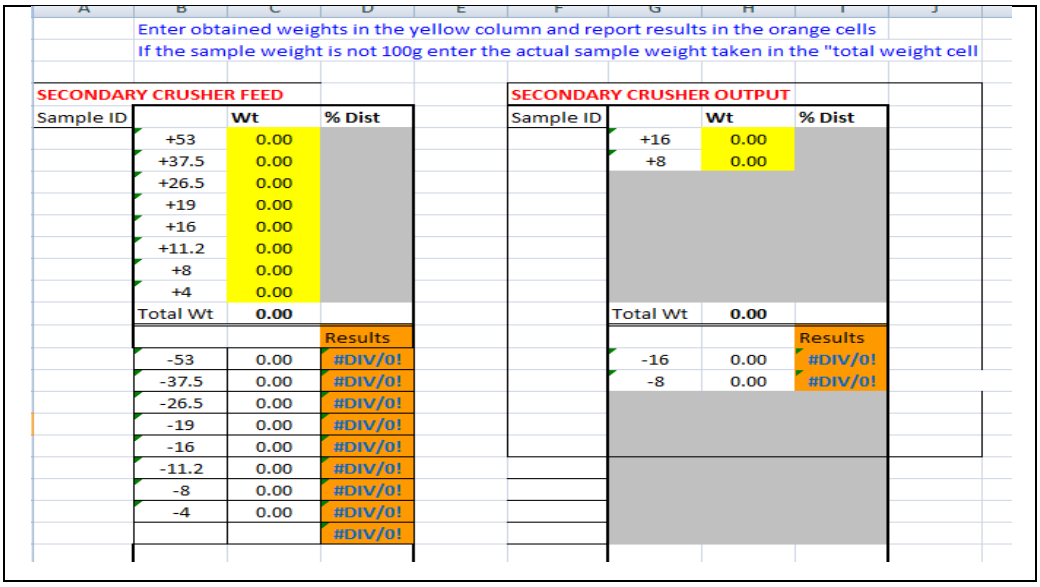

Enter obtained weights in the yellow column and report results in the orange cells
If the sample weight is not 100g enter the actual sample weight taken in the "total weight cell

SECONDARY CRUSHER FEED

Sample ID		Wt	% Dist
	+53	0.00	
	+37.5	0.00	
	+26.5	0.00	
	+19	0.00	
	+16	0.00	
	+11.2	0.00	
	+8	0.00	
	+4	0.00	
	Total Wt	0.00	
			Results
	-53	0.00	#DIV/0!
	-37.5	0.00	#DIV/0!
	-26.5	0.00	#DIV/0!
	-19	0.00	#DIV/0!
	-16	0.00	#DIV/0!
	-11.2	0.00	#DIV/0!
	-8	0.00	#DIV/0!
	-4	0.00	#DIV/0!
			#DIV/0!

SECONDARY CRUSHER OUTPUT

Sample ID		Wt	% Dist
	+16	0.00	
	+8	0.00	
	Total Wt	0.00	
			Results
	-16	0.00	#DIV/0!
	-8	0.00	#DIV/0!

Figure 3.9 PSD work sheet image

3.2.3 Specific Gravity of Ore

The specific gravity of a rock material is determined strictly as the ratio of a mass of a volume of a material at a stated temperature to the mass of the same volume of distilled water at a stated temperature (ASTM, 2000). Table 3.4 below describes the apparatus used in this experiment.

Table 3.4 Equipment used in ore SG determination

Equipment	Specification
Container	250 ml Beaker
Water	Distilled water
Weighing Scale	Metler Toledo SB24001, Max 24100g, e= 1g, Min 5g, d= 1g/.1g

Under measured room temperatures of 26℃ the following steps were taken to determine the ore specific gravity after a belt cut:

1) Weigh the container and note down the container weight (m_1)
2) Fill the container with distilled water and weigh container with distilled water (m_2)
3) Dry the container and fill it up with dry ore and obtain the weight (m_3)

(2) and (3) are illustrated in figure 3.10

Calculate the Specific gravity (S.G) using equation 3.5:

$$S.G = \frac{m_3 - m_1}{m_2 - m_1} \quad (3.5)$$

Figure 3.10 Weight of beaker with distilled water and beaker with ore

For statistical analysis purposes the procedure was repeated five times and obtained data captured on an excel spreadsheet depicted in figure 3.11.

Title: SPECIFIC GRAVITY WORKSHEET | Ref No:- ACM-LAB-FRM-021

DATE: _____ FILE NAME: _____

Sample type: _____ Analysis Type: _____

Lab No	Wt Of Empty Cont m1	Wt Of Cont + Sample m3	Wt Of Cont + Dist Water m2	Dry Wt of sample m3 -m1	Dist water Weight m2 -m1	Specific Gravity
1				0.00	0.00	#DIV/0!
2				0.00	0.00	#DIV/0!
3				0.00	0.00	#DIV/0!
4				0.00	0.00	#DIV/0!
5				0.00	0.00	#DIV/0!
6				0.00	0.00	#DIV/0!

Weighed by : _____ Date:

Figure 3.11 SG work sheet image

3.3 CONE CRUSHER POWER DRAW EXPERIMENTS

In order to answer research question number two, experiments were carried out on the secondary crusher to determine the relationship between the crusher power draw and the crusher cavity level and the ore feed rate. In this exercise, the belt weigher was calibrated and an ultrasonic transmitter was installed and calibrated to measure the crusher cavity level. As illustrated in figure 3.12 and figure 3.13, power logger was hooked onto the crusher motor phases in the MCC.

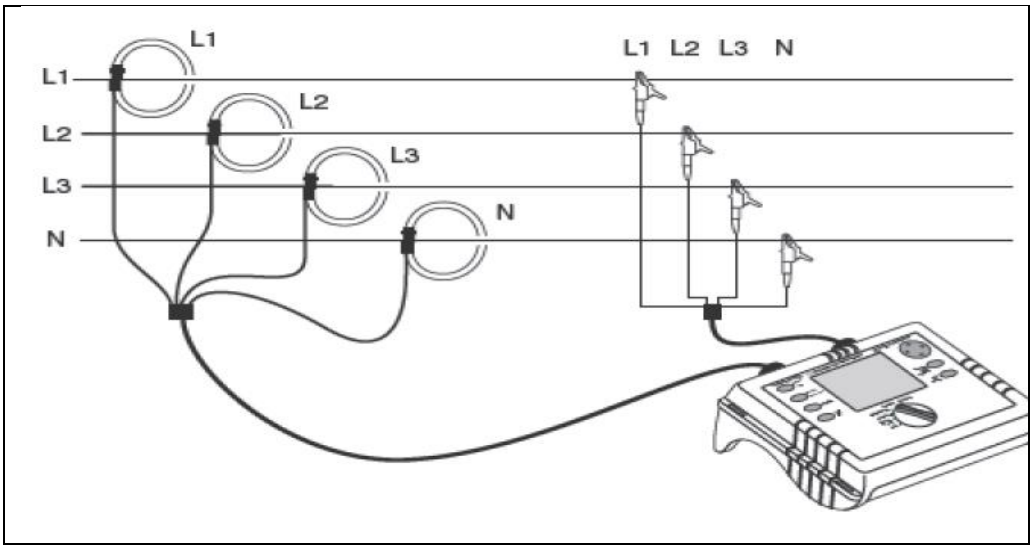

Figure 3.12 Three phase measurement (Fluke Corporation, 2008)

Figure 3.12 shows the three phase measurement on the secondary crusher switchgear and the screen shot of the Fluke meter display.

Figure 3.13 Power Logger connections and the display screenshot

For data acquisition, an engineering station loaded with Mitsubishi PLC and ADROIT SCADA software programs was hooked to the plant

PLC/SCADA network via the Moxa Ethernet switch and placed next to the power logger.
Data collected in these experiments was captured on Excel spreadsheets for statistical analysis.

Table 3.5 illustrates the equipment used in this exercise and their specifications.

Table 3.5 Equipment used in Power Draw experiments

Equipment	Specification
Level Transmitter	VEGA61 Ultrasonic level transmitter
Power Logger	Fluke 1735 Power Logger
Belt weigher Integrator	Mini 11-101F Thermo electron Integrator
SCADA	ADROIT version 8.0
PLC	Mitsubishi Q series (GX IEC Developer 7.01)
Cone Crusher Motor	WEG 260Kw,525V,340A,1490rpm
Cone Crusher	Osborn 57S gyrasphere cone crusher

The secondary crusher, with open circuit configuration was used to ensure consistent feed properties. The tests took a period of four days, as to allow for production between the experiments. All crusher parameters were kept constant with the exception of the investigated parameters. For Mowana mine the power draw experiments were limited to level and feed rate versus power draws since the crushers are configured to run at a constant preset *CSS* and fixed *ES.*

3.3.1 Power draw versus Ore feed rate

Crusher power variation was achieved by varying the speed reference output to the VSD for the pan feeders which feed onto the crusher feed conveyor. The federate into the crusher was an input to the PLC from a Microtech 101 weight meter as depicted in figure 3.14 below.

Figure 3.14 Power draw versus ore feed rate experimental setup

For experimental management purpose the following steps were taken:

1) Set the *CSS* to 16 mm
2) Noted the *ES* of the crusher
3) Connected the Fluke 1735 Power Logger in Delta connection as shown in figure 3.12 with the rotary switch selected to power measurement mode
4) Ran the crusher circuit empty and noted the power draw
5) Increased the feeder speed gradually till a steady feed rate was attained (in steps of 0,100,150,200,250,300,350 tons per hour) and noted the power draw at each respective feed rate
6) Repeated the experiment five times for statistical analysis purposes

The results of the crusher feed rate versus the power draw were captured and backed up on an excel spreadsheet and a regression analysis of the

results was carried out to determine the relationship between the two parameters.

3.3.2 Power draw versus Crusher Cavity level

Crusher power variation was achieved by varying the speed reference output to the VSD for the pan feeders which feed onto the crusher feed conveyor. The ore level in the crusher cavity was an input to the PLC and SCADA from an ultrasonic level transmitter and the setup is depicted in figure 3.15.

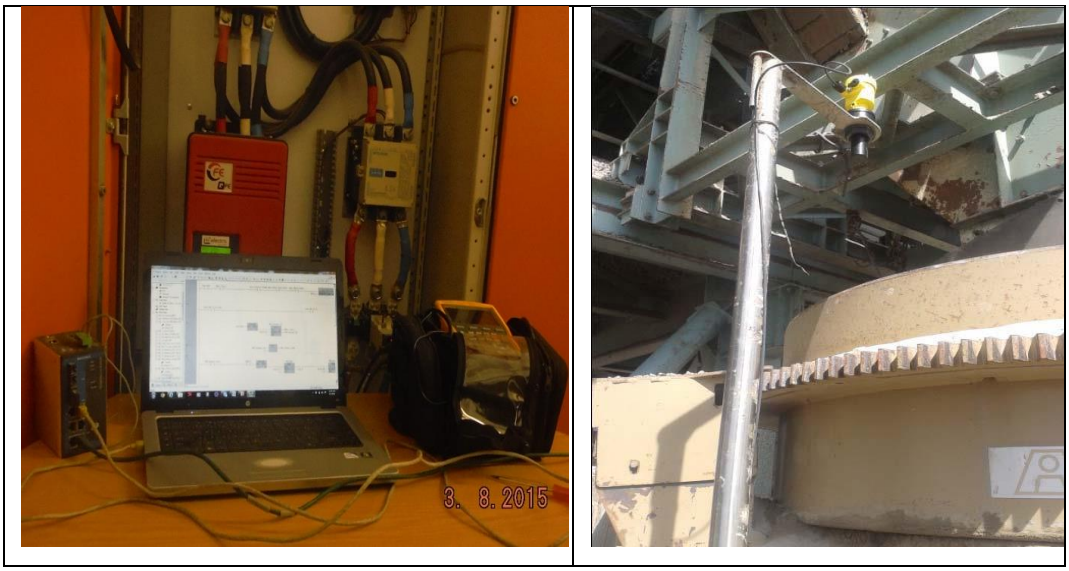

Figure 3.15 Power draw versus cavity level experimental setup

For experimental control purposes the following steps were followed:

1) Set the CSS to 16 mm
2) Noted the ES of the crusher

3) Connected the Fluke 1735 Power Logger in Delta connection as shown in figure 3.12 with the rotary switch selected to power measurement mode
4) Ran the crusher circuit empty and noted the power draw at zero cavity level
5) Increased the feeder speed gradually till a fairly steady cavity level reading was attained (in steps of 0,25,50,75,100 percent) and noted the power draw at each respective cavity level.
6) Repeated the experiment five times for statistical analysis purposes

The results of the level and the associated power draw were captured and backed up on an excel spreadsheet and a regression analysis of the results was carried out to determine the relationship between the two parameters.

3.4 SIMULATION AND OPTIMISATION PROCEDURE

In designing a dynamic simulator for the crushing circuit optimization purposes, the following steps were taken:

1) The Mowana mine cone crusher was presented as the Whiten perfect model
2) A mass balance was performed around the crusher
3) Modelled the vibrating screen as a static system and constant speed conveyors as a time delay
4) Evaluated the Mowana crusher model. Determined its breakage and classification matrices using the Broadbent and Callcott method
5) Equipped with the breakage and classification matrices, simulated the effect of disturbances on the product PSD using Matlab® .
6) Simulated for disturbances (PSD, SG, M, FSD and Q) on the Mowana crushing circuit by varying the disturbances in step form.

Each disturbance was varied one at a time and taken back to its nominal value.

7) Simulated for controllable parameters (CSS and ES) to determine if they have more influence on the process than the disturbances, hence checking for process controllability.
8) Designed a control system using a dynamic simulation on a Matlab®/Simulink® and the PLC and SCADA platform for optimisation purposes.
9) Tuned the power controller PID parameters using the Ziegler – Nichols tuning rules.
10) Simulated the response of the controller to disturbances using an electric motor with a VSD controlled braking system and a gearbox as a load.

3.4 ERROR ANALYSIS

In this research work, an error analysis is conducted in order to analyse the reliability of the presented results. Several factors originate errors and uncertainty in the results, of special mention being sensor calibration errors, power versus level or feed rate estimation models, parameterization errors, measurement errors of the sensors and data acquisition hardware, and the errors of linear regression models. This section seeks to analyse the quantities of these errors and present a propagation of uncertainty for every measurement signal and result.

3.5.1 Calibration and Parameterisation Errors

The calibration and parameterisation errors originated from the inaccuracies of manual measurements performed in this research work. Manual measurements were performed in the initial setting up and calibration of the ultrasonic level sensor, ES determination, CSS measurement, and in the level/power draw parameterisation. Pulley diameters and lead pieces were measured by a Vernier calipers whilst the

height setup of the crusher cavity level sensor was determined using a tape measure. Initial calibration and parameterisation errors are presented in table 3.6.

Table 3.6 Sources of Calibration and Parameterisation Errors

Parameter	Value	Error
Installation height of the level transmitter	1.10m	±0.01m
Pulley diameter Measurements (motor and driven)	345.00mm	±0.05mm
	720.00mm	±0.05mm

Calibration and parameterisation errors in this research were minimised by calibrating the transmitters following standard procedures stipulated in the instrument manual. As for all manual measurements, average values were used after repeated measurements followed by a statistical analysis of the obtained results.

3.5.2 Measurement Errors

The magnitude of the measurement error is dependent on the internal accuracy of the instrument being used as well as the measurement method. In this research a belt weigher is of major concern since it is used as a reference for all the belt cuts and ore feed rate. All the quantitative results presented in this work are affected by the error the belt weigher generates. The Thermoelectron Micro 101 belt weigher manual declared an accuracy of ±1%, whilst the real error could be worsened by the lack of periodic calibrations. At Mowana mine an accuracy of ±2.5 % is set for all the weight meters.

Errors generated by manual measurements have the most significant effect to the measurement signals of the ultrasonic level measurement system, pulley diameter measurements and lead pieces measurement in determining the crusher. These parameters are inputs to the developed models. In this research measurement errors were minimised by having more than one experienced individual carryout repeated measurements followed by a statistical analysis of the presented measurements. Only mean values were used.

The accuracies of sensors used in this research are listed in table 3.7.

.**Table 3.7** The accuracies of sensors used

Parameter	Accuracy
Ultrasonic level sensor	± 0.2%
Belt scale	± 2.5%
Top pan scale	± 0.1%
Power logger	± 0.5%

3.5.3 Data acquisition and linear regression Errors

Errors due to data acquisition hardware and linear regression are estimated to be very small and cannot be reliably estimated. In this research work the errors due to data acquisition were left out in the uncertainty calculations of the performed measurements. Errors generated by the linear regression method are related to the calculation accuracy of the software used for linear parameter estimation. Due to the automatic nature of the linear regression method applied, the errors are considered to be low. This error could have been included in the uncertainty calculation if the linear regression parameters were estimated manually.

In this research the quantisation errors were minimised by the use of belt load continuous integrators for weight measurement and a PLC and a SCADA system which filters low level signals quantisation errors due the high measurement frequency (500Hz) .Noise in the signals transmission was reduced by the use of the data bus between PLC Modules and the CPU. In a data bus signals are digitized to minimise and rectify transmission errors.

CHAPTER 4 MODELLING THE PERFORMANCE OF THE MOWANA CRUSHING PLANT

This chapter presents the results of the laboratory experimental program conducted to characterise the ore properties. The results enable one to understand and model the breakage behaviour of the ore within the operation of the Mowana mine crushing plant.

4.1 CRUSHER CLOSED SIDE SETTING

The crusher closed side setting (*CSS*) of the secondary crusher was calculated based on the information provided by two analysts here labelled BN and TS. Five replicates were collected by both technicians on the secondary crusher. The data is reported in Table 4.1.

Table 4.1 Set of *CSS* measurements by the two analysts (BN and TS)

BN		TS	
Samples	Measurement (mm)	Samples	Measurement (mm)
Run1_16_BN	16.05	Run1_16_TS	16.10
Run2_16_BN	16.20	Run2_16_TS	16.20
Run3_16_BN	15.80	Run3_16_TS	16.00
Run4_16_BN	17.10	Run4_16_TS	17.20
Run5_16_BN	16.05	Run5_16_TS	16.10

Table 4.2 Statistics extracted from the *CSS* data

	BN data	TS data
Mean (mm)	16.24	16.32
Standard Error	0.224	0.222
Standard Deviation	0.502	0.497
Sample Variance	0.252	0.247
Minimum	15.80	16.00
Maximum	17.10	17.20
Count	5	5
Confidence Level (95 %)	0.623	0.617

The descriptive statistics for the two datasets, i.e. BN and TS, are reported in Table 4.2. The mean *CSS* values were found to be 16.24 ± 0.22 mm and 16.32 ± 0.22 mm respectively from BN and TS. On performing a Fischer's test (F-test) in Microsoft Excel© for a one-tailed F-critical, the findings were as reported in Table 4.3.

Table 4.3 F-test for BN and TS datasets

	BN	TS
Mean	16.29	16.38
Variance	0.321	0.309
Observations	4	4
Degree of freedom	3	3
F	1.03706	
F-critical one-tail	9.27663	

From Table 4.3, since F < F-critical at 95 % confidence level, there is statistically no significant difference between the two datasets, i.e. BN and TS. It can therefore be stated that the differences observed between the two datasets are due to random error.

The two datasets were combined and the global mean *CSS* calculated. The value obtained was found to be *CSS* = 16.33 ± 0.22 mm. This is the final average value of CSS considered later as input to the crusher model.

4.2 CRUSHER ECCENTRIC SPEED

Based on the physical gear counts of the secondary crusher, the following values were obtained: pinion gear teeth $T_1 = 21$ and bevel gear teeth $T_2 = 62$.

The average values from the calliper measurements of pulley diameters d_2 and d_1 were used. From Figure 3.3, the measured driven pulley was verified through the following calculation: $n_2 = \frac{n_1 \times d_1}{d_2} = \frac{1475 \times 345}{720} = 706.8$ rpm. This is in the range of the average speed determined by the tachometer; hence, the speed from the tachometer was used for the calculation of the eccentric speed (*ES*).

Since the speeds of the driven pulley and the pinion gear are the same but in countershaft, $n_3 = 707.08$ rpm. The main shaft and eccentric speed can be determined from Equation (3.1): $n_4 = \frac{n_3 \times T_1}{T_2} = \frac{707.08 \times 21}{62} = 239.47 \pm 0.05$ rpm.

The *ES* of the secondary crusher was calculated to be 239.47 ± 0.05 rpm. This value was later used as an input value to the crusher model.

4.3 ORE SPECIFIC GRAVITY

From the crusher product samples, a sample was collected for the ore specific gravity analysis. The data collected was captured on an electronic worksheet as shown in Figure 4.1. This information was then processed in Microsoft Excel©; the statistics extracted thereafter is reported in Table 4.4.

Title: SPECIFIC GRAVITY WORKSHEET | Ref No:- ACM-LAB-FRM-021

DATE: _29-07-15 | FILE NAME: SG_Thakadu_290715

Sample type: Crusher Product | Analysis Type: SG

Lab No	Wt Of Empty Cont m1	Wt Of Cont + Sample m3	Wt Of Cont + Dist Water m2	Dry Wt of sample m3 -m1	Dist water Weight m2 -m1	Specific Gravity
1	87.60	628.34	285.90	540.74	198.30	2.73
2	88.10	634.25	286.70	546.15	198.60	2.75
3	87.80	644.46	285.90	556.66	198.10	2.81
4	87.70	625.53	284.80	537.83	197.10	2.73
5	87.80	644.46	285.90	556.66	198.10	2.81
6	88.10	633.73	286.70	545.63	198.60	2.75

Weighed by : K. Kahirindi | Date: 29/07/15

Figure 4.1 Raw data collected from the specific gravity test

Table 4.4 Statistics extracted from the specific gravity data

Mean	2.762
Standard Error	0.0156
Standard Deviation	0.0382
Sample Variance	0.0014
Minimum	2.727
Maximum	2.810
Count	6
Confidence Level (95 %)	0.0401

The specific gravity of the ore being fed into the crusher was determined to be 2.762 ± 0.016. This average value together with the CSS value found in the previous section is later used as inputs to the crusher model.

4.4 ORE MOISTURE

The initial data collected during the moisture analysis of the ore being fed to the crusher is shown Figure 4.2.

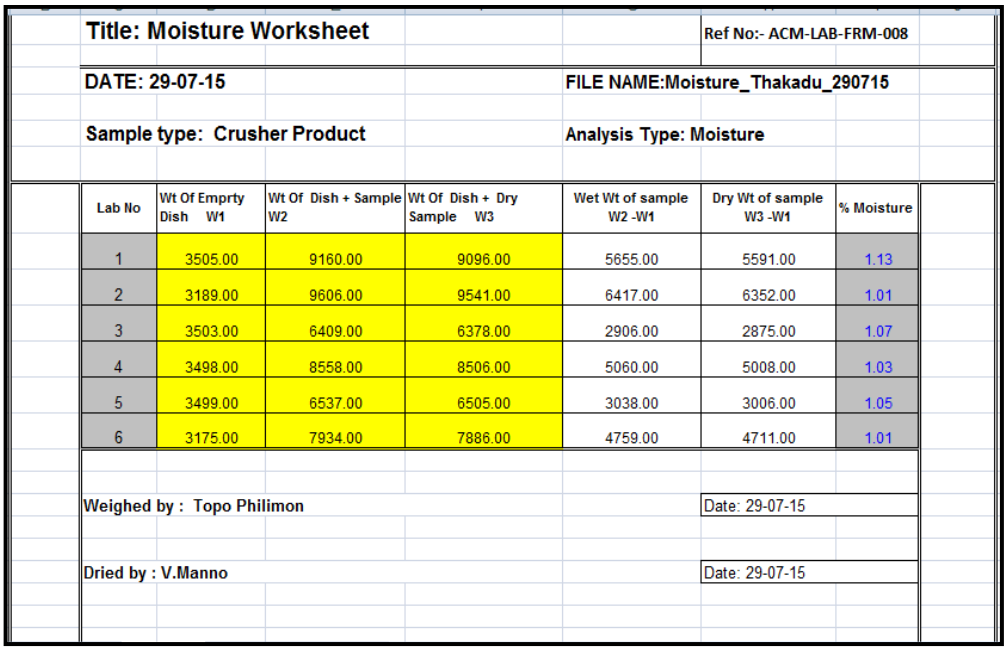

Title: Moisture Worksheet — Ref No:- ACM-LAB-FRM-008

DATE: 29-07-15 — FILE NAME:Moisture_Thakadu_290715

Sample type: Crusher Product — Analysis Type: Moisture

Lab No	Wt Of Emprty Dish W1	Wt Of Dish + Sample W2	Wt Of Dish + Dry Sample W3	Wet Wt of sample W2 -W1	Dry Wt of sample W3 -W1	% Moisture
1	3505.00	9160.00	9096.00	5655.00	5591.00	1.13
2	3189.00	9606.00	9541.00	6417.00	6352.00	1.01
3	3503.00	6409.00	6378.00	2906.00	2875.00	1.07
4	3498.00	8558.00	8506.00	5060.00	5008.00	1.03
5	3499.00	6537.00	6505.00	3038.00	3006.00	1.05
6	3175.00	7934.00	7886.00	4759.00	4711.00	1.01

Weighed by : Topo Philimon — Date: 29-07-15

Dried by : V.Manno — Date: 29-07-15

Figure 4.2 Ore moisture data

Like in the previous two sections (4.2 and 4.3), the data was analysed statistically. The outcome of this endeavour is summarised in Table 4.5.

Table 4.5 Results from the moisture content test

Mean (%)	1.050
Standard Error	0.0188
Standard Deviation	0.0459
Sample Variance	0.0021
Minimum	1.009
Maximum	1.132
Count	6
Confidence Level (95 %)	0.04823

The moisture content of 1.050 ± 0.019 % was found in the ore being fed into the secondary crusher. This average value is also later used as input parameter to the crusher model.

4.5 FEED SIZE DISTRIBUTION

In order to determine the particle size distribution (PSD) of the ore feed to the crusher, two analysts collected separate samples and performed a size analysis. The two analysts (here labelled LN and TT) were used to validate the sampling technique and extracted the level of accuracy of the data. The two sets of data are provided in Tables 4.6 and 4.7.

Table 4.6 Particle size analysis: Reference LN

01-Conv-01			
Screen size (mm)	Mass (g)	Retained (%)	Passing (%)
75.0			100
53.0	12 316	36.6	63.4
37.5	5 154	15.3	48.1
26.5	2 911	8.6	39.5
19.0	2 499	7.4	32.0
16.0	1 168	3.5	28.6
11.2	2 177	6.5	22.1
8.0	1 452	4.3	17.8
4.0	2 351	7.0	10.8
-4.0	3 637	10.8	
Total	33 665		
Belt speed:	2 m/s	Date:	27/08/15
Distance:	1 m	Time:	14:30
Throughput:	242 t/h	Analyst:	L. Ndlovu

Table 4.7 Particle size analysis: Reference TT

01-Conv-01			
Screen size (mm)	Mass (g)	Retained (%)	Passing (%)
75.0			100
53.0	18 963	40.9	59.1
37.5	4 249	9.2	49.9
26.5	3 799	8.2	41.7
19.0	2 236	4.8	36.9
16.0	986	2.1	34.8
11.2	1 908	4.1	30.7
8.0	1 601	3.5	27.2
4.0	3 372	7.3	19.9
-4.0	9 249	19.9	
Total	46 363		
Belt speed:	2 m/s	Date:	27/08/15
Distance:	1 m	Time:	12:00
Throughput:	334 t/h	Analyst:	T. Tsepho

Next, an F-test for a one-tailed F-critical was performed in Microsoft Excel©. The findings are presented in Table 4.8.

Table 4.8 F-test results for the pair of PSD data

	LN	TT
Mean	32.75	37.63
Variance	286.786	157.696
Observations	8	8
Degree of freedom	7	7
F	1.81859	
F-critical one-tail	3.78704	

Based on the statistics in Table 4.8, it can be seen that F < F-critical at 95 % confidence level. As a result, it can be said that the difference observed between the pair of PSD data, i.e. LN and TT, is due to random error. The PSD results by LN are arbitrarily taken as input to the crusher model.

To complement the feed size distribution data, the crusher product was also sampled. The motivation behind this was to determine the crusher efficiency at the time of feed sampling.

Table 4.9 Particle size distribution of the crusher product

02-Conv-01			
Screen size (mm)	Mass (g)	Retained (%)	Passing (%)
75.0			100
53.0	0	0.0	100
37.5	0	0.0	100
26.5	0	0.0	100
19.0	132	0.3	99.7
16.0	200	0.5	99.2
11.2	4 901	12.3	86.9
8.0	10 012	25.0	61.9
4.0	10 762	26.9	35.0
-4.0	13 996	35.0	
Total	40 003		
Belt speed:	0.6 m/s	Weightometer tonnage: 80 t/h	
Distance:	1 m	Mass variance: 0.49 %	
Throughput:	86 t/h	Throughput variance: 7.4 %	

The size distribution data of the crusher product is reported in Table 4.9. It can be seen that 99 % of the product passes through a screen of aperture 16.0 mm. This size is close enough to the *CSS* = 16.33 ± 0.22 mm found in Section 4.2 to warrant confidence in the *CSS* value reported.

4.6 MODELLING POWER DRAW AS A FUNCTION OF CAVITY LEVEL

The data pertaining to the effects of crusher cavity level on power draw is summarised in Table 4.10. Recall that the collection procedure for this data is described in Section 3.3.2.

It can be seen from the results listed in Table 4.10 that an increase in cavity level incurs a proportional increase in power draw, the power factor, and the root mean square current. Note here that the power factor improves with increased cavity level. This means the electrical energy supplied to the crusher is efficiently converted into the mechanical work that creates the rotation and nutation of the crusher.

Table 4.10 Results for power draw as a function of cavity level

Cavity level (%)	Active power (kW)	Power factor (-)	V_{rms} (V)	I_{rms} (A)
0	51.31	0.71	532.3	80.1
25	91.08	0.72	532.6	129.8
50	129.40	0.73	531.8	187.6
75	161.78	0.77	530.4	216.4
100	209.07	0.81	531.2	273.8

A regression analysis was performed to determine the relationship between the crusher variables, the active power draw and the cavity level. To do this, the active power was set as the dependent variable whilst the cavity level was the independent variable. The regression analysis then was carried out with the primary objective to determine the best set of parameters from a least-square point of view.

The outcome of this effort is present graphically in Figure 4.3. Note a coefficient of determination of $R^2 = 0.9972$ which signifies that no less than 99.72 % of the active power data can be explained with the proposed linear correlation:

$$Active\ power = (1.5449 \times Cavity\ level) + 51.2840 \quad (4.1)$$

Equation 4.1 is therefore accepted to be a good representative of the relationship between crusher cavity level and active power.

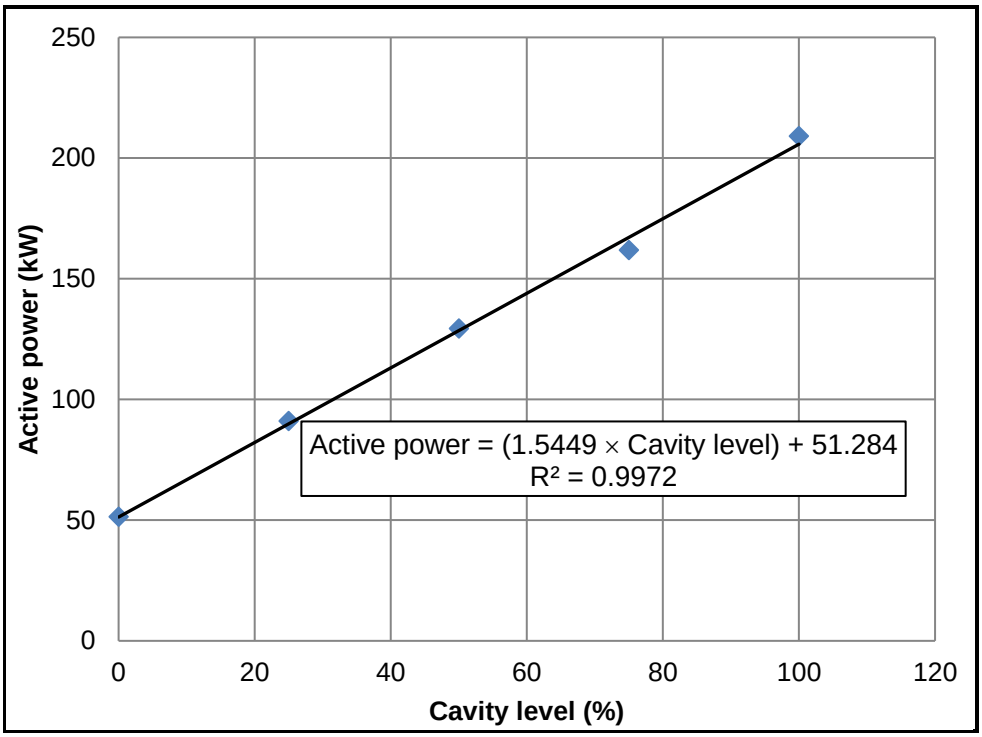

Figure 4.3 Linear fit describing active power versus cavity level

Furthermore, a low regression standard error of 3.75% as illustrated in figure 4.4 proves a linear fit between the crusher power and its cavity level.

Regression Statistics	
Multiple R	0.998600043
R Square	0.997202045
Adjusted R Square	0.996269394
Standard Error	3.735105532
Observations	5

Figure 4.4 Regression Statics for active power versus cavity level

From this analysis, it can be concluded that since there is a linear relationship between the two crusher variables, they can be considered in the design of the linear crusher controller.

4.7 MODELLING POWER DRAW AS A FUNCTION FEED RATE

The results obtained from the experiment of the active power draw are presented in Table 4.11. For reference, the data collection protocol is described in Section 3.3.1.

A note similar to that made in the previous section is that the power factor improves as feed rate increases. However, further loading of the crusher would lead to adverse stoppages and downtimes which are the motivation behind the present work. So, although crushing overloading seems to be attractive in terms of improved power factor, its implementation is severely restricted.

Table 4.11 Active power draw measured at different feed rates

Feed rate (tph)	Active power (kW)	Power factor (-)	V_{rms} (V)	I_{rms} (A)
0	80.10	0.71	532.4	53.01
100	138.47	0.73	532.0	95.21
150	152.87	0.76	531.7	102.85
200	183.58	0.76	531.1	131.43
250	213.77	0.77	531.0	159.18
300	252.65	0.78	530.7	176.96
380	266.60	0.80	530.0	196.27

A statistical analysis similar to that presented in Section 4.6 was carried out in order to come up with a relationship between the active power draw and feed rate to the crusher. The result is illustrated in Figure 4.4.

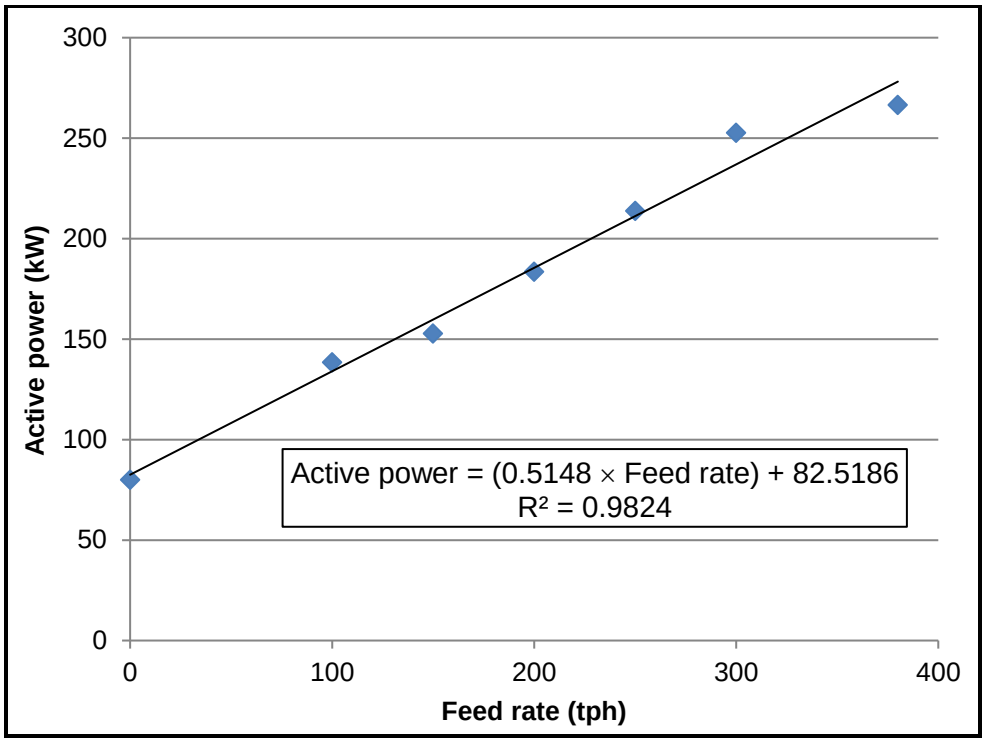

Figure 4.5 Linear fit describing active power versus ore feed rate

With a coefficient of determination of $R^2 = 0.9824$, it can be concluded that the active power draw at a given feed rate is given by:

$$Active\ power = (0.5148 \times Feed\ rate) + 82.5186 \quad (4.2)$$

Equation 4.2 shows that there is a linear relationship between the two crusher variables; that is why, the two variables are considered later in the design of the crusher controller.

Furthermore, a regression standard error of 9.61% reveals that there is a linear relationship between the crusher power and the federate. It is about three times bigger than that of the crusher active power and its cavity level mainly because of the wildness of flow in any form by nature. This error can be easily managed by the introduction of a finely tuned PID controller.

Regression Statistics	
Multiple R	0.991162898
R Square	0.982403891
Adjusted R Square	0.978884669
Standard Error	9.613961722
Observations	7

Figure 4.6 Regression Statistics for active power versus ore feed rate

4.8 SUMMARISED FINDINGS

The chapter presented the outcome from the Mowana mine site laboratory experimental programs which were carried out to characterise the ore and crusher properties. The properties are to be used as inputs to models and simulations to be carried out in this research work.

A regression analysis was carried out to determine the relationship between two sets of crusher variables namely: active power versus the cavity level and power draw versus feed rate into the crusher. The statistical analysis resulted in the equations 4.1, demonstrating the linear relationship between the crusher active power to the cavity level, and equation 4.2, also displaying the linearity between the crusher power draw and feed into the crusher. The two sets of crusher parameters will be considered in the design of the cone crusher PID controllers.

CHAPTER 5 SIMULATION AND OPTIMISATION OF THE MOWANA CRUSHING PLANT

This chapter outlines the undertakings carried out at Mowana Mine during the year 2014 to 2016 in order to design a dynamic simulator for control purposes. The simulator incorporates a library of equipment which was blended to configure a crushing stage.

The crushing plant components are coupled by a flow of material with the following elements: solid mass flow rate, particle size distribution, and ore hardness.

5.1 DYNAMIC MODELLING OF THE MOWANA CRUSHING PLANT

The principal constituents of the Mowana crushing circuit are stockpiles, bins, conveyor belts, screens, and crushers. In modelling of the Mowana crushing plant conveyor belts, screens, and cone crushers were considered.

5.1.1 Dynamic model of the cone crusher

The cone crusher model used in the simulator as well as the affiliated variables is illustrated in Figure 5.1. The model is based on the Whiten perfect model covered in Chapter 2.

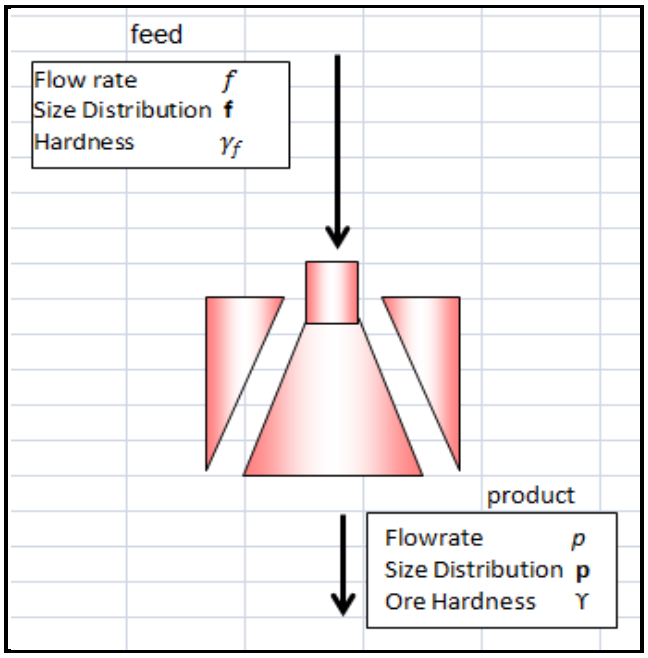

Figure 5.1 The cone crusher model and its main variables

By performing a mass balance around the crusher, the following can be obtained:

$$\frac{dm(t)}{dt} = f(t) - p(t) - \gamma(t)(S - B\,S)\,m(t) \tag{5.1}$$

where $\gamma(t)$ is a variable representing the ore hardness

$\boldsymbol{f}(t)$ and $\boldsymbol{p}(t)$ are vectors having elements $\boldsymbol{f}_i(t)$ and $\boldsymbol{p}_i(t)$, which are the mass flow rate in the ith fraction of the feed and the product respectively

$\boldsymbol{S}$ is the diagonal matrix representing the specific breakage of particles of size i

$\boldsymbol{B}$ is the lower diagonal matrix, where B_{ij} represents the fraction of particles of size fraction j appearing in the fraction size i after breakage

The steady-state solution of Equation 5.1 is Equation 2.5 which is found by setting the first term to zero and expressing $\boldsymbol{p}(t)$ in terms of $\boldsymbol{f}(t)$.

5.1.2 The model of the cone crusher screen

The vibrating screen was modelled as a static system since there is no dynamic associated with such equipment. As illustrated in Figure 5.2, the undersize $\boldsymbol{p}_u$ and oversize $\boldsymbol{p}_o$ are given by the relationship (Sbárbaro, 2010):

$$p_u = (I - C)\, f \tag{5.2}$$

$$p_o = C\, f \tag{5.3}$$

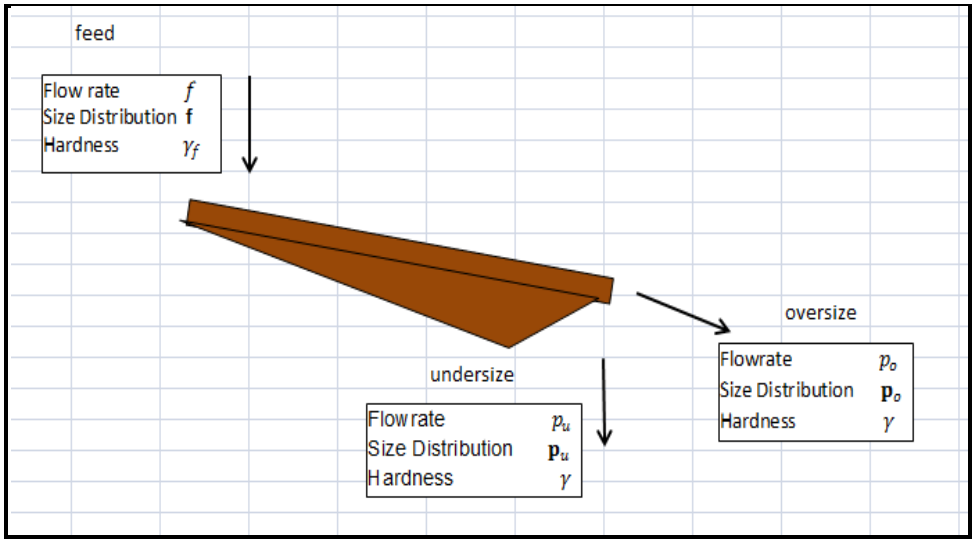

Figure 5.2 The Screen and its main variables

5.1.3 The model of the constant-speed conveyors

The conveyor belts were modelled as a sheer time delay as illustrated in Figure 5.3.

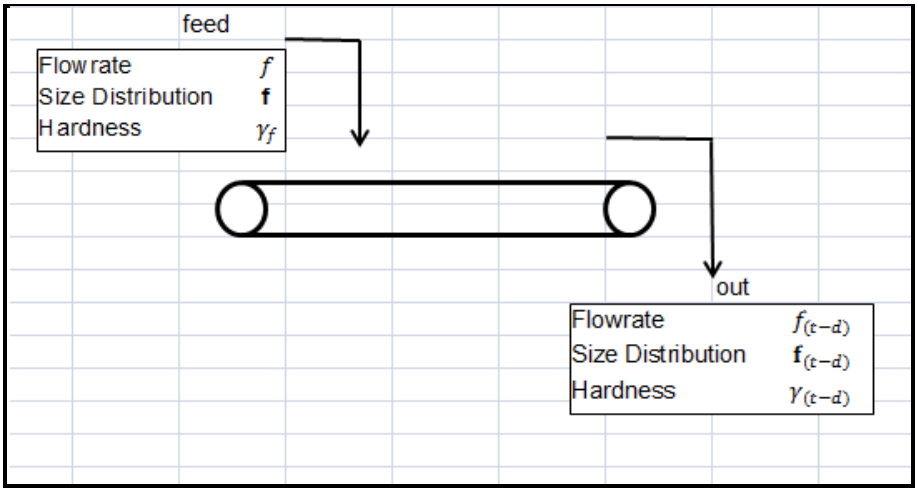

Figure 5.3 The constant speed conveyor and its main variables

The product from the conveyors is expressed as follows:

$$p(t) = f(t-d) \tag{5.4}$$

where $\boldsymbol{p}$ is the conveyor product.

5.2 MODEL OF ORE SIZE REDUCTION

In order to describe the Mowana crushing operation mathematically, the mass balances at the feed and product ends were derived from Equation 2.5. The product P from and the feed F to the crusher were obtained experimentally whereas the breakage function B and the classification function C were evaluated as described below.

5.2.1 Evaluation of the Mowana crusher model

In order to build the Mowana crusher model following the Whiten framework, two matrices are needed: the breakage and classification matrices. Their determination necessitated the data presented in Table 4.9 and Table 5.1.

Table 5.1 Size distribution of the crusher product

Interval	-	1	2	3	4	5	6
Size, µm	20500	19000	16000	11200	8000	4000	-4000
% Retained	-	0.3	0.5	12.3	25.0	26.9	35.0

The method proposed by Broadbent and Callcott was used as far as the breakage function is concerned. It is expressed as follows (Gupta and Yan 2006):

$$B(d_i) = \frac{1-\exp(-d_i/d_j)}{1-\exp(-1)} \qquad (5.5)$$

$B(d_i)$ is the proportion of material of initial size d_j that is less than size d_i in the product while size d_j refers to the top size of the interval.

The initial size d_1 is the geometric average particle size for the top fraction (-20500 +19000 µm): $d_1 = \sqrt{20500 \times 19000}$ = 19735µm.

From Equation 5.5 and for i = 1, $d_i = d_j$ and $B(d_1) = 1$.

For i = 2, $B(d_2) = \frac{1-\exp(-d_2/d_1)}{1-\exp(-1)} = \frac{1-\exp(-19000/19735)}{1-0.36788} = 0.978$

Similar calculations as those described above were done for other values of i. The results are summarised in Table 5.2.

Table 5.2 The proportion of the material size versus the top size interval

Size Interval	d_i	$B(d_i)$
1	19735	1.000
2	19000	0.978
3	16000	0.879
4	11200	0.685
5	8000	0.527
6	4000	0.290

Since $B(d_i)$ is the proportion less than the size d_i, the proportion broken into size d_i is obtained by subtracting $B(d_i)$ from $B(d_{i-1})$ or from 1 in the case of the top size; that is,

B(1, 1) = 1 – 0.978 = 0.022

B(2, 1) = 0.978 – 0.879 = 0.099

B(3, 1) = 0.879 – 0.685 = 0.194

B(4, 1) = 0.685 – 0.527 = 0.158

B(5, 1) = 0.527 – 0.290 = 0.237

B (6, 1) = $1-\sum_{i=1}^{i=5} B(i,1)$ = 0.290. It is the material broken into size interval 6, which is less than 4000 μm.

Table 5.3 The Mowana mine crusher B matrix

Size Interval	d_i	$B(d_i)$	B(i, j)
1	19735	1.000	0.022
2	19000	0.978	0.099
3	16000	0.879	0.194
4	11200	0.685	0.158
5	8000	0.527	0.237
6	4000	0.290	0.290

From Table 5.3, the breakage matrix can be written in the form that follows (size class i = 6 is not included):

$$B = \begin{bmatrix} 0.022 & 0 & 0 & 0 & 0 \\ 0.099 & 0.022 & 0 & 0 & 0 \\ 0.194 & 0.099 & 0.022 & 0 & 0 \\ 0.156 & 0.194 & 0.099 & 0.022 & 0 \\ 0.237 & 0.158 & 0.194 & 0.099 & 0.022 \end{bmatrix}$$

The matrix for the feed $\boldsymbol{f}$ and product $\boldsymbol{p}$, from Table 4.7 and Table 4.9 respectively are as follows:

$$f = \begin{bmatrix} 40.9 \\ 9.2 \\ 8.2 \\ 4.8 \\ 2.1 \end{bmatrix} \quad \text{and} \quad p = \begin{bmatrix} 0.0 \\ 0.0 \\ 0.0 \\ 0.3 \\ 0.5 \end{bmatrix}$$

From Equation 2.5, it follows that: $P[I - BC] = [I - C]F$ where

$$C = \begin{bmatrix} C_{11} & 0 & 0 & 0 & 0 \\ 0 & C_{22} & 0 & 0 & 0 \\ 0 & 0 & C_{33} & 0 & 0 \\ 0 & 0 & 0 & C_{44} & 0 \\ 0 & 0 & 0 & 0 & C_{55} \end{bmatrix}$$

Finally, it can be deduced that $C_{11}=1$, $C_{22}=1$, $C_{33}=1$, $C_{44}=0.939$, and $C_{55}=0.779$.

$$C=\begin{bmatrix}1 & 0 & 0 & 0 & 0\\ 0 & 1 & 0 & 0 & 0\\ 0 & 0 & 1 & 0 & 0\\ 0 & 0 & 0 & 0.939 & 0\\ 0 & 0 & 0 & 0 & 0.779\end{bmatrix}$$

5.3 SIMULATION OF THE MOWANA CRUSHING CIRCUIT

The controllability and correlative out-turn of feed material disturbances were examined for the Mowana mine crushing plant. The simulated feed material disturbances and manipulated variables were assigned pragmatic ranges derived from the experimental data with an assumption that the simulated parameters were only exposed to natural variations.

5.3.1 Effects of disturbances on Product

Equipped with the breakage and classification matrices applicable to the Mowana cone crusher, the effect of disturbances on the product PSD was determined in Matlab® as illustrated below:

In this simulation, all vector and matrices were converted to their polynomial form for the final graphical simulation results (refer to Matlab® in Appendix A). Figure 5.4 is the outcome of the endeavor.

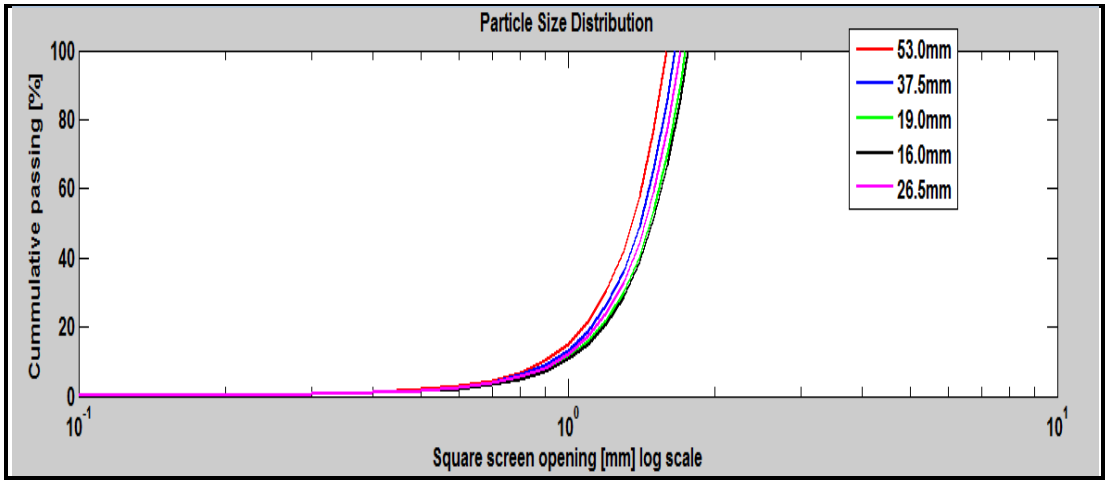

Figure 5.4 Simulation 1: Effects of all disturbances on product size distribution

Figure 5.4 outlines the worst case scenario of all the possible input parameter combined on the product size distribution PSD. The maximum PSD can be achieved with maximum specific gravity SG, minimum ore moisture M, maximum feed size distribution FSD and minimum feed rate Q. whereas the minimum PSD can be obtained with the reverse set of these parameters.

5.3.2 Dynamics of the cone crusher

The models determining the crusher and material flow dynamics were derived from Equations 2.8 and 2.9. A summary of these models is presented in Table 5.4.

Table 5.4 A summary of the Mowana mine Capacity and Power models

Ore Fed Crusher	Capacity Model	Power Model
Input: Disturbances (Feed material) Input: Controllable parameters (ES & CSS)	$\frac{1}{0.25T_d\ s+1}$	$\frac{1}{(0.5T_d\ s+1)(0.25T_d\ s+1)}$

In Table 5.4, T_d is the material residence time in the crusher and is estimated by $\frac{CZ}{ES}\times 60$ with CZ: the number of crushing zones and ES: the crusher eccentric speed. For the cone crusher at the Mowana mine, $T_d = 0.64\,\text{min}$.

5.3.3 Simulating the disturbances

Amongst the numerous factors influencing the crushing circuit operation at the Mowana mine, feed size distribution (FSD), ore moisture (M), specific gravity (SG) and feed rate (Q) have been studied in the previous chapters.

In this chapter, simulation strategies were resorted to. During the simulation for the disturbances caused by selected operating parameters, a particular variable is adjusted independently, by effecting step changes from the nominal operating point. Following testing for both high and low values, the corresponding parameter is reset to its nominal value. The effect of each variable is related to the process output (crusher power and capacity) at nominal conditions. An identical procedure is carried out for the CSS and ES input variables.

It should be noted that due to the non-linearity of the system, the outcome is expected to be influenced by the chosen operating point. The nominal

operating points were selected with an objective of giving realistic ranges for variables as much as possible. The chosen nominal, minimum and maximum input values are tabulated in Table 5.5.

Table 5.5 Nominal, minimum and maximum input values for simulations

	TESTED VARIABLE		**Nominal**	**Min**	**Max**	**Nom %**
Case 1	Moisture	***M***	1	0.1	3	31
Case 2	Feed Rate, mass flow in	***Q***	100 %	34 %	70 %	100
Case 3	Specific Gravity	***SG***	2.7	2.6	2.8	50
Case 4	Feed Size Distribution	***FSD***	30 mm	4 mm	75 mm	48
Case 5	Closed side setting	***CSS***	16 mm	14 mm	19 mm	40
Case 6	Eccentric Speed	***ES***	240 rpm	200 rpm	370 rpm	23

Simulations were executed for disturbances (case 1 to 4) and the other for controllable parameters. The Simulink® simulation layout is presented in Figure 5.5. A variation is made during the simulation, of plugging in the transfer functions for the secondary crusher from Table 5.4 with $T_d = 0.64\,\text{min}$ for the crusher capacity and power respectively.

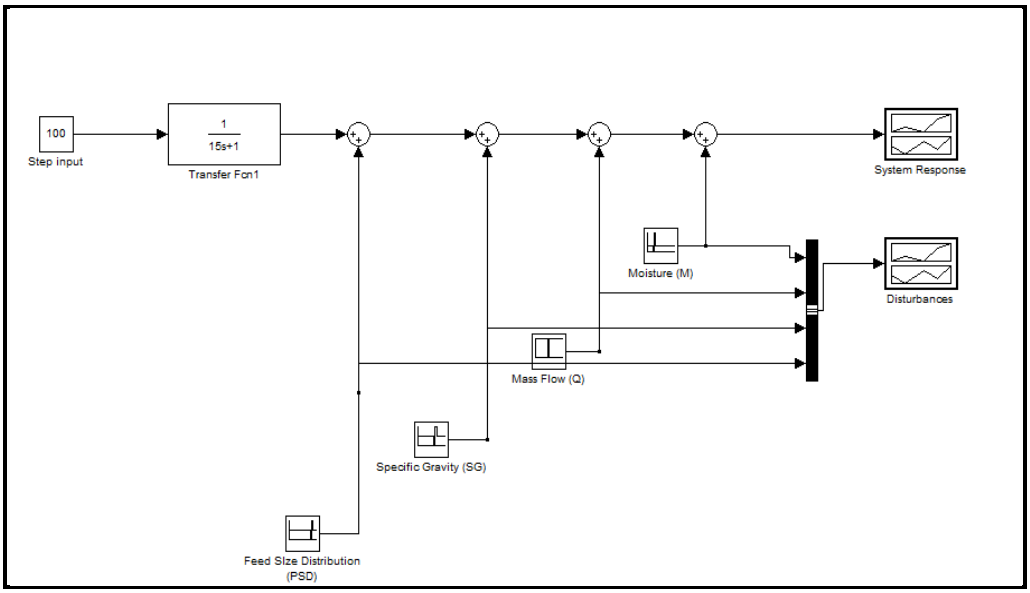

Figure 5.5 Simulation model for the effects of disturbances on crusher power or capacity

Input signals for these simulations are illustrated in Figures 5.6 and 5.7.

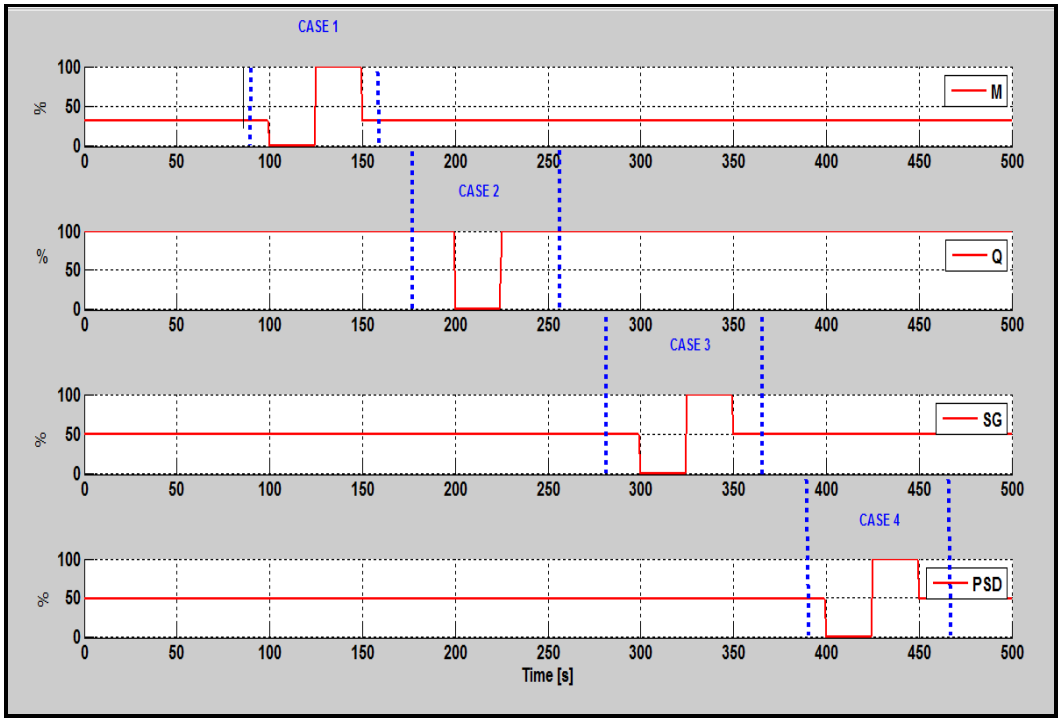

Figure 5.6 Input sequence for disturbances simulation

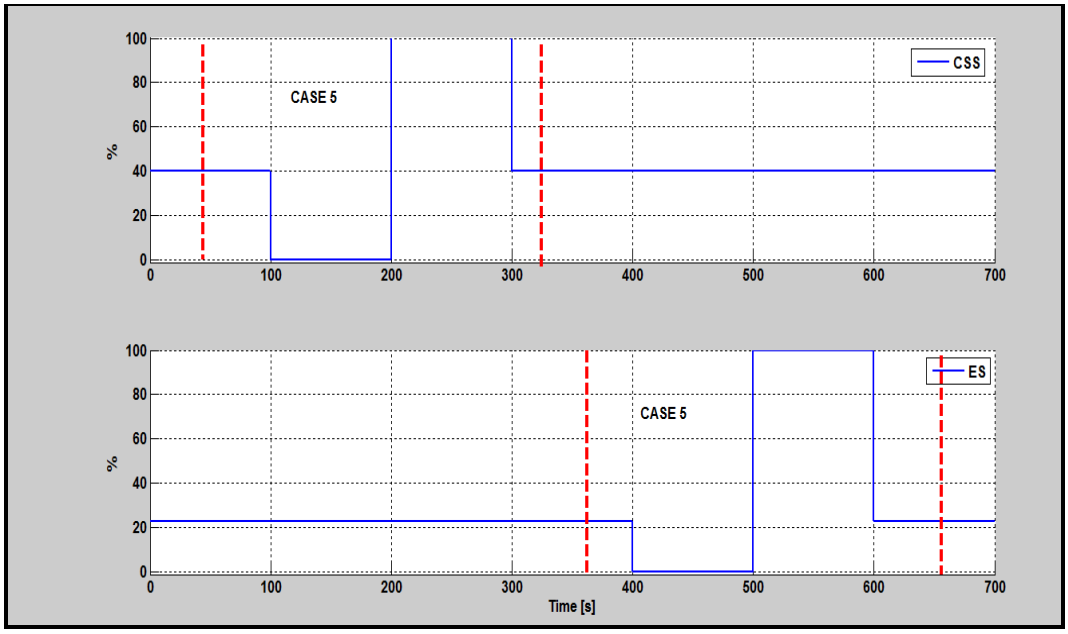

Figure 5.7 Input sequence for controlled variables simulation

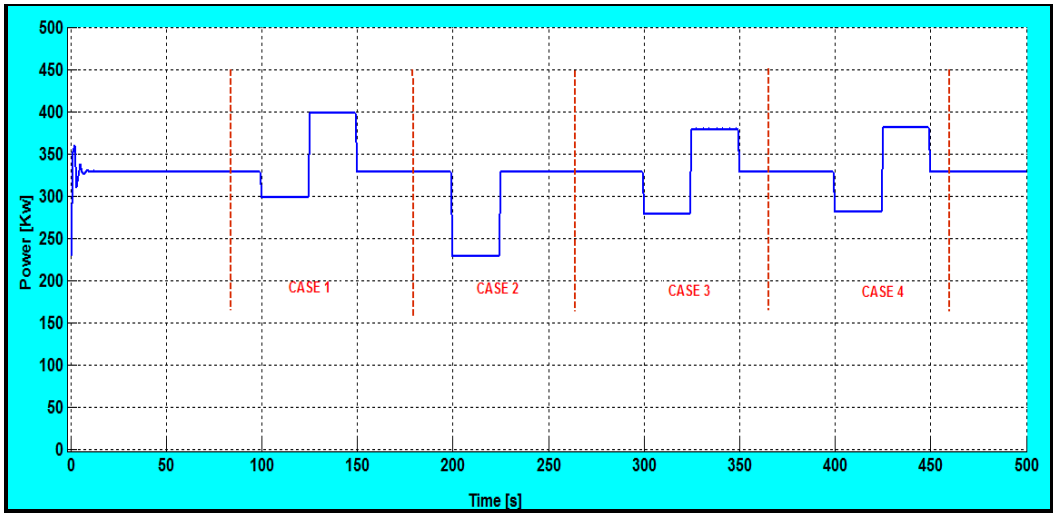

Figure 5.8 Effects of disturbances on the crusher crushing power

The response from the simulation of disturbances is shown in Figures 5.8 and 5.9. It can be seen that the simulated disturbances have resembling dynamics except for feed rate. The observation is indicative of the plug flow pattern of the ore fed into the cone crusher; the result is a static relationship between the crusher input and output. Note that it is less probable that the step-like disturbances would be obtainable in the real crushing plant process.

Conversely, the feed rate does not follow the same pattern as that of the rest of the simulated conditions. This may be due to the fact that its dynamics is dependent on the ratio between mass flow in and mass flow out.

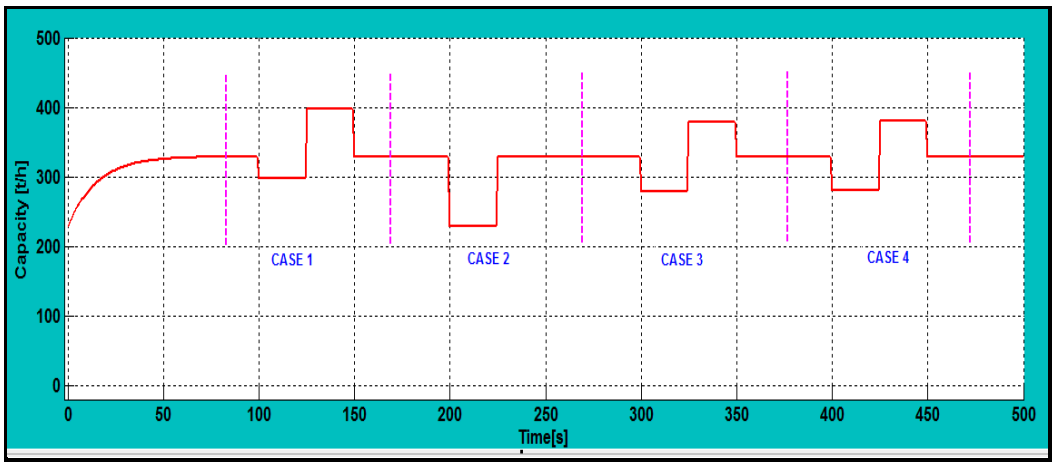

Figure 5.9 Effects of disturbances on the crusher capacity

It also appears the influence of feed material on crushing power is negligible while moisture and feed size distribution show marked alterations in the crushing power.

All in all, visual observation shows M and FSD are the most influential disturbances. It is also noticeable that the ore feed rate can influence the crusher capacity and crushing power on ranges between zero and the nominal values.

5.3.4 Simulation 3: Controllable parameters

Figure 5.10 presents the effect of controllable parameters simulation in Simulink® on the cone crusher.

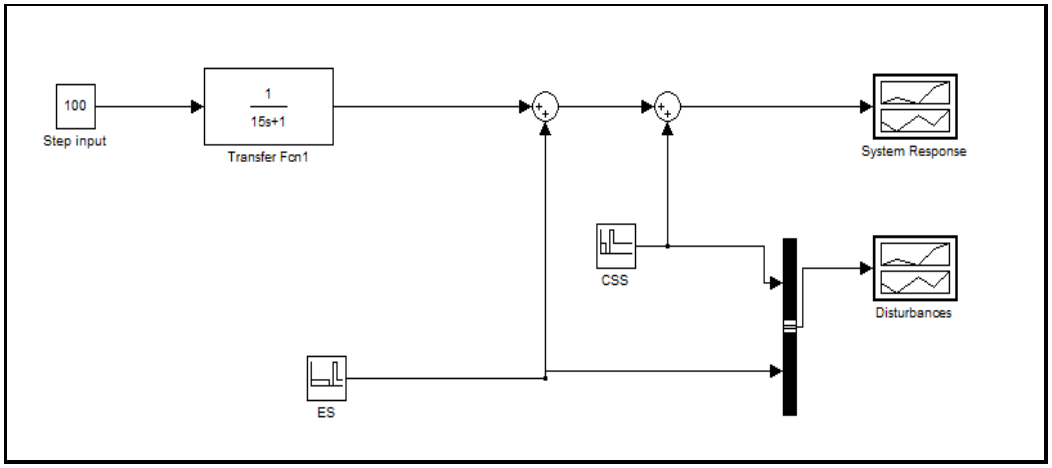

Figure 5.10 Simulation 3: Controllable parameters

The response from the simulation of disturbances is provided in Figures 5.11 and 5.12.

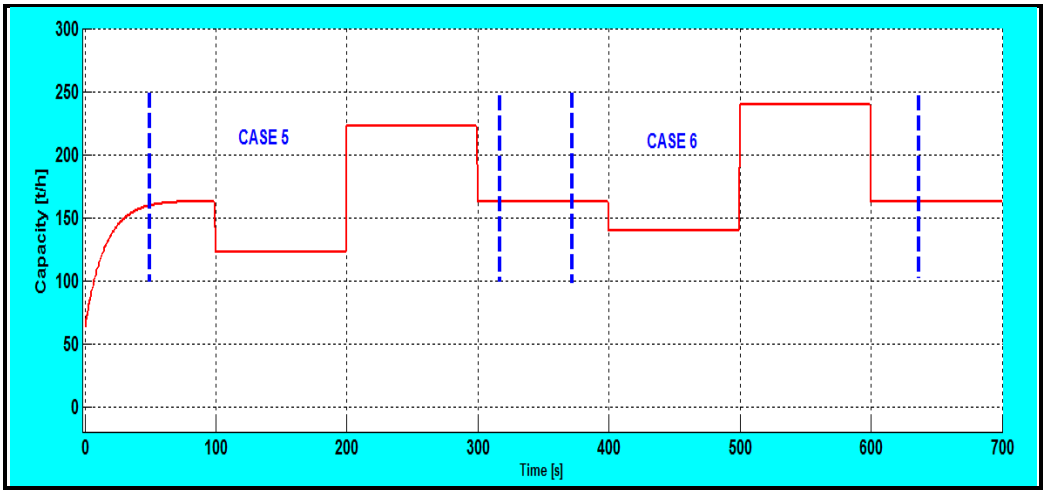

Figure 5.11 Effects of controlled variables on the crusher capacity

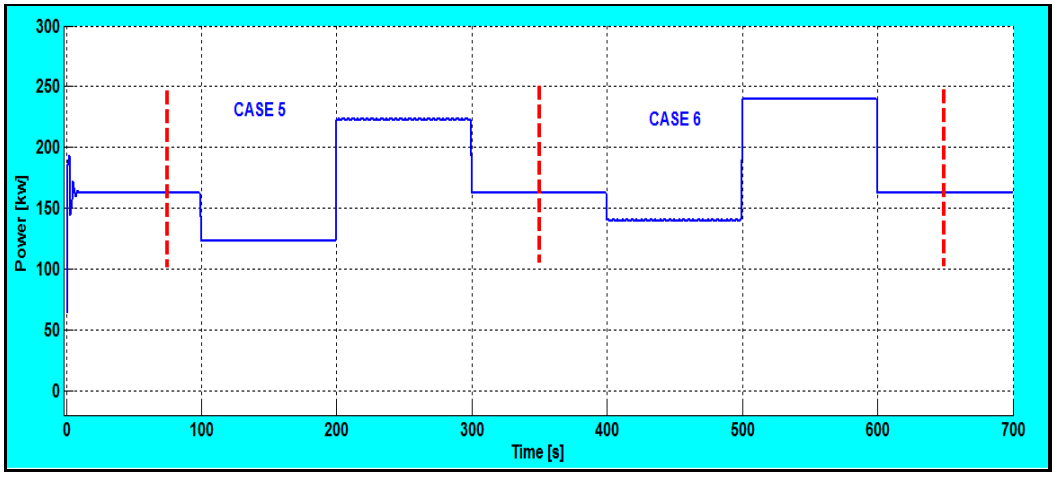

Figure 5.12 Effects of controlled variables on the crushing power

According to the simulations conducted, the dynamics of *ES* are similar to the dynamics of *CSS*. Of the two, the crusher *CSS* is the most influential control variable.

5.4 OPTIMISATION OF THE SECONDARY CRUSHING CIRCUIT

A control system was designed to regulate feed rate using a dynamic simulation. The system was developed and optimised before its implementation at the Mowana secondary crushing section. This was performed using Matlab®/Simulink® and the PLC and SCADA platform stationed at the mine.

5.4.1 Tuning the crusher power controller

The crusher power transfer function is $P(s) = \frac{1}{(0.32\,s+1)(0.16\,s+1)}$. The control system in Figure 5.13 represents the non-choke feed conditions for the power model. The transfer function of the PID controller is $G_c(s) = K_p\left(1 + \frac{1}{T_i\,s} + T_d\,s\right)$.

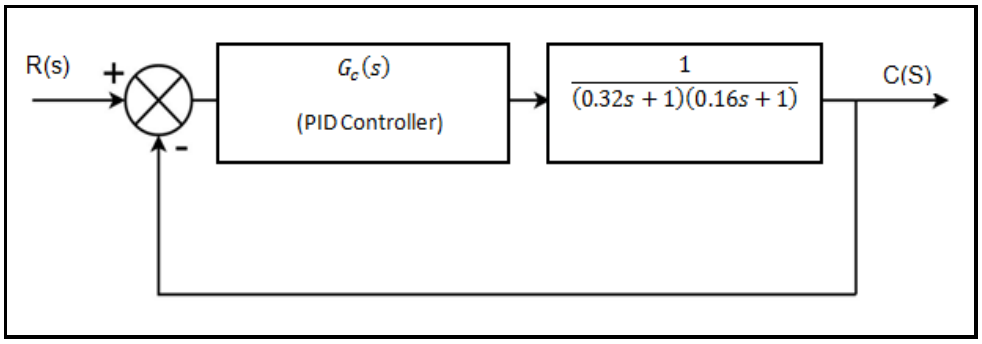

Figure 5.13 The block diagram for the PID controlled power model

The overall transfer function was calculated with the application of the Ziegler-Nichols tuning for the determination of parameters K_p, T_i and T_d in mind. It given by $\frac{C(s)}{R(s)} = \frac{K_p}{K_p + (0.32\,s+1)(0.16\,s+1)}$.

The value of K_p that makes the system marginally stable so that sustained oscillations occur can be obtained by Routh's stability criterion. Since the characteristic equation for the closed loop system is:

$$0.05\,s^2 + 0.48\,s + 1 + K_p = 0$$

The Routh array becomes an illustration in Table 5.6.

Table 5.6 Routh table

S^2	0.05	1	0
s^1	0.48	K_p	0
s^0	$\frac{0.48 - 0.05\,K_p}{0.48}$	0	0

Examining the coefficients of the first column of the Routh table reveals that sustained oscillations will occur if $K_p = 9.6$. Thus, the control gain $K_{cr} = 9.6$ and the characteristic equation is $0.05\,s^2 + 0.48\,s + 10.6 = 0$.

To find the frequency that sustains the oscillation, substitute $s = \sqrt{-1}\,\omega$ into this characteristic equation: $0.05\left(\sqrt{-1}\,\omega\right)^2 + 0.48\left(\sqrt{-1}\,\omega\right) + 10.6 = 0$. Equate the real terms: $\omega = \pm 14.56$ rad/s. Hence, the period corresponding to sustained oscillations is $P_{cr} = \frac{2\pi}{\omega} = 0.43$.

The following can also be derived: $K_p = 0.6K_{cr} = 5.76$; $T_d = 0.125P_{cr} = 0.054$; and $T_i = 0.5P_{cr} = 0.215$. The transfer function of the PID controller is thus

$$G_c(s) = K_p\left(1 + \frac{1}{T_i\,s} + T_d\,s\right) = 5.76\left(1 + \frac{1}{0.215\,s} + 0.054\,s\right)$$

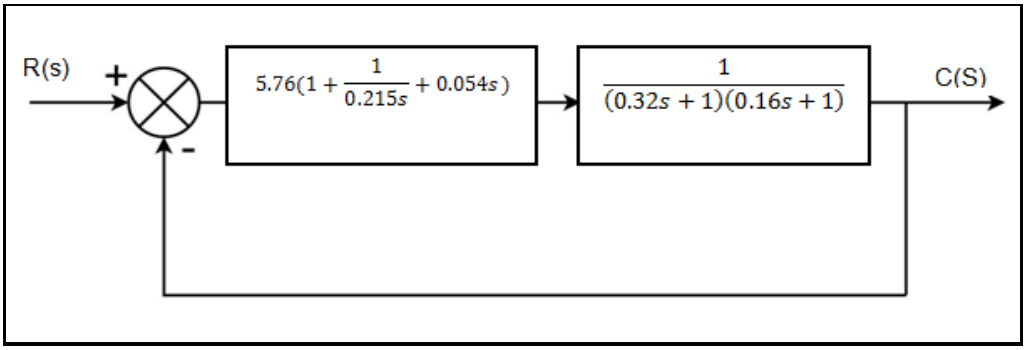

Figure 5.14 Block diagram of the loop with PID controller designed by use of Ziegler-Nichols tuning rule

From Figure 5.14, it can be deduced that

$$G(s)G_c(s) = 5.76\frac{(0.012\,s^2+0.215\,s+1)}{(0.011\,s^3+0.103\,s^2+0.2151\,s)}$$

A step input in the transfer function above can now be introduced using Matlab® with the setup shown in Figure 5.15.

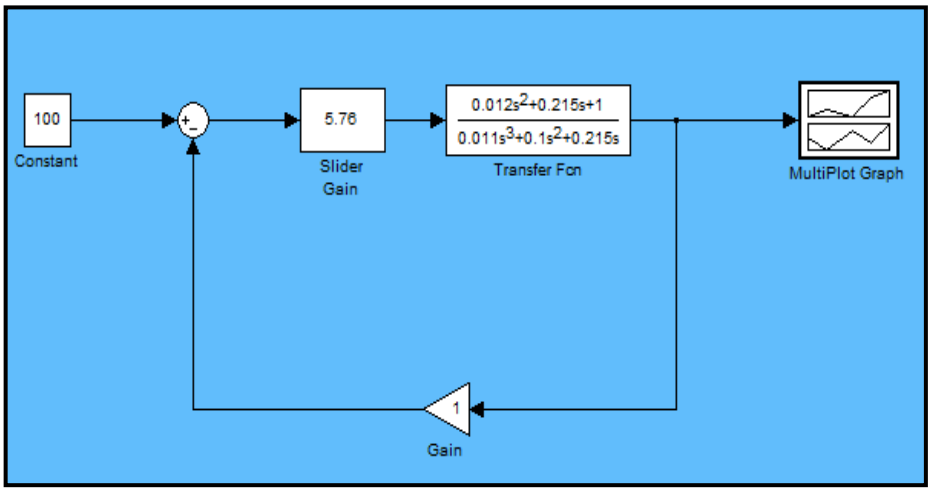

Figure 5.15 Matlab® block diagram representation of the simulation

The response to a step unit of 100 (feed simulation) is illustrated in Figure 5.16.

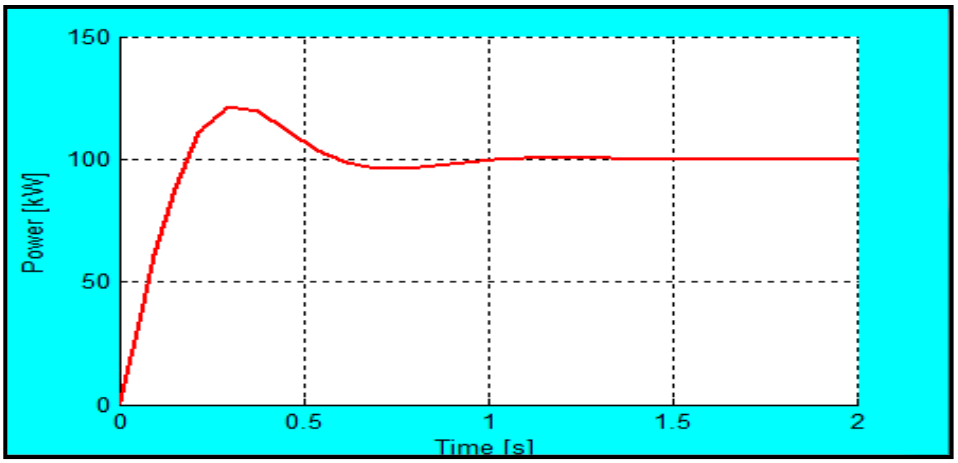

Figure 5.16 System's response with a step input

The response plot shows that the Ziegler-Nichols settings have achieved the one-quarter amplitude damping, but however the overshoot is approximately 18.5 %. Fine-tuning the controller using the root locus follows.

The closed loop transfer function of the system becomes

$$\frac{C(s)}{R(s)} = \frac{0.069\,s^2 + 1.238\,s + 5.760}{0.011\,s^3 + 0.790\,s^2 + 1.453\,s + 5.760}$$

The root locus of the closed-loop transfer function above can now be generated as shown in Figure 5.17. It can be seen that the value of K_p which brings the overshoot of closest to 0 % is 31.7.

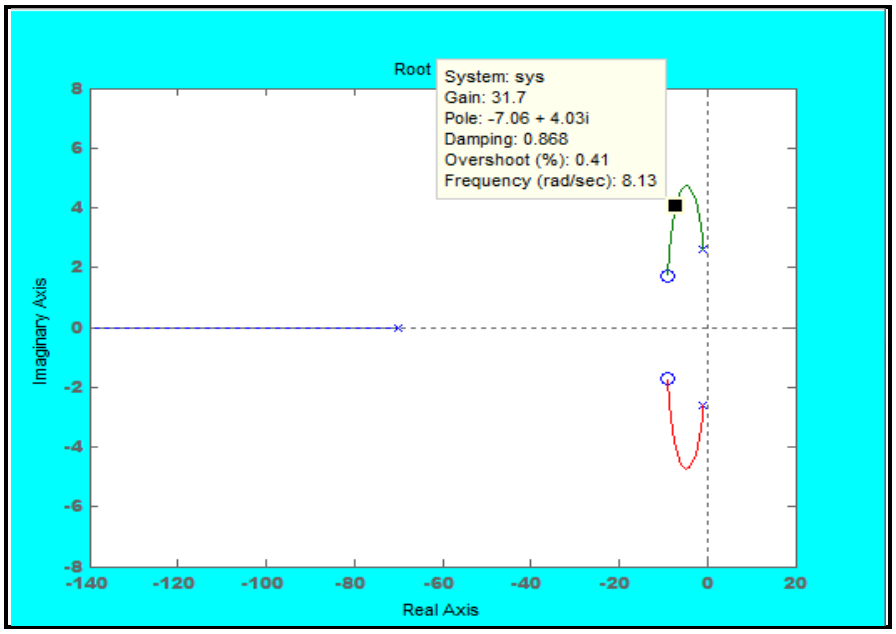

Figure 5.17 Root locus plot of system with Ziegler-Nichols of the PID controller

The selected parameters of the power model controller with all disturbances equated to zero with the exception of one parameter which was feed into the crusher are tabulated in Table 5.7.

Table 5.7 The crusher power controller PID values

Controller Term	Value
P	31.7
T_i	0.215 s
T_d	0.054 s

For the cavity level controller the plant existing PID terms were selected and are tabulated in Table 5.8.

Table 5.8 The cavity level controller PID values

Controller Term	Value
P	60
T_i	1600 s
T_d	Off

5.4.2 The Mowana crushing circuit simulator

An optimal control model which utilises the power draw and cavity level of the cone crusher as well as a self-tuning control algorithm, at PLC and SCADA level of control was developed as depicted in Figure 5.18.

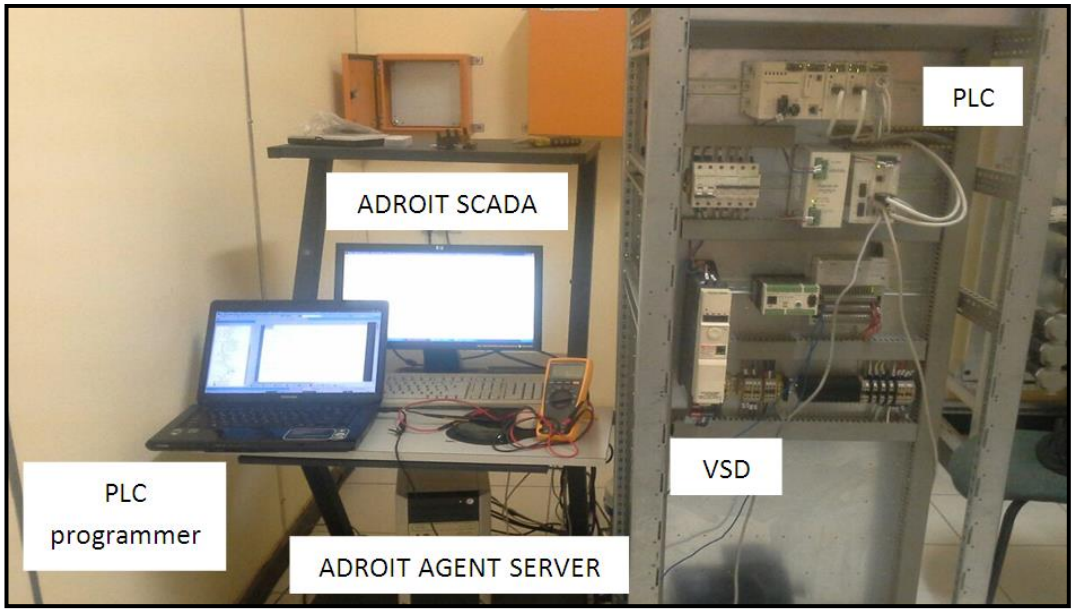

Figure 5.18 The PLC control model for crusher circuit optimization

The simulator consists mainly of two machines: one running the PLC program and the other running as the Adroit agent server with an HMI (Human Machine Interface) displaying the developed crushing circuit mimic, all in a network with the PLC. The variable speed drive is to vary the speed of the feeder to the crusher. Since it was not practical to hook up the simulator to the real crushing plant, an electric motor with a braking system and a gearbox with no load were used in lieu of the crusher for simulation purposes. The electric motor was run at a constant speed with

a current transformer and a current to 4 to 20 mA convertor monitoring the current drawn by the motor hence the power draw. Instead of the feeder being manipulated the braking system will vary the load in proportion to the error generated. The motor wand gearbox setup with a braking system is depicted in Figure 5.19.

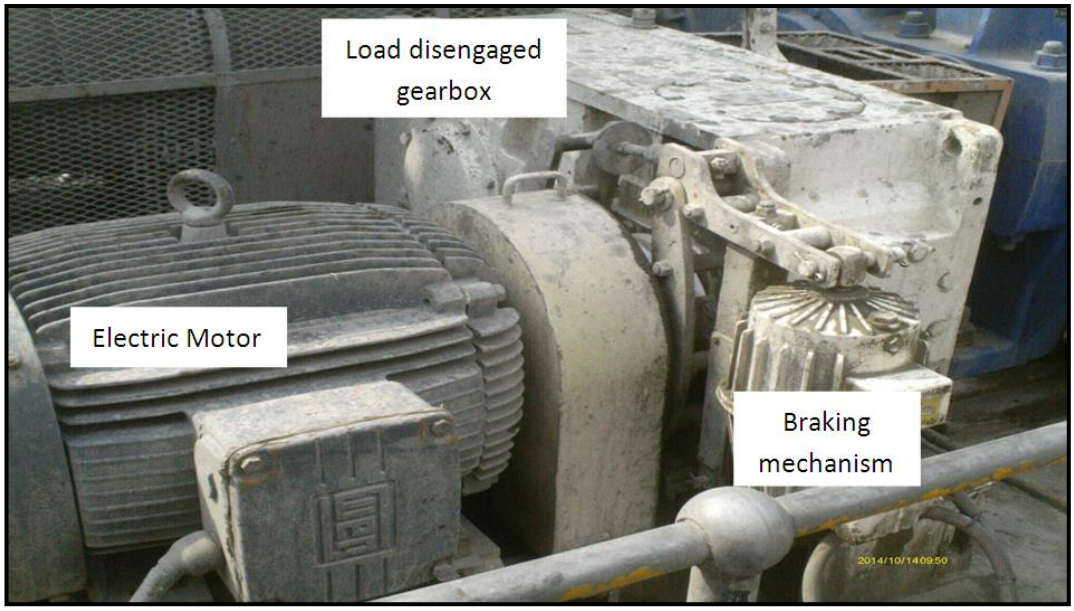

Figure 5.19 Motor coupled to a no-load gearbox with a VSD controlled braking system

The self-tuning controller using two variables, power draw and cavity level is depicted in Figure 5.20. The set points and PID parameters can be changed from the SCADA system or directly on the PLC program.

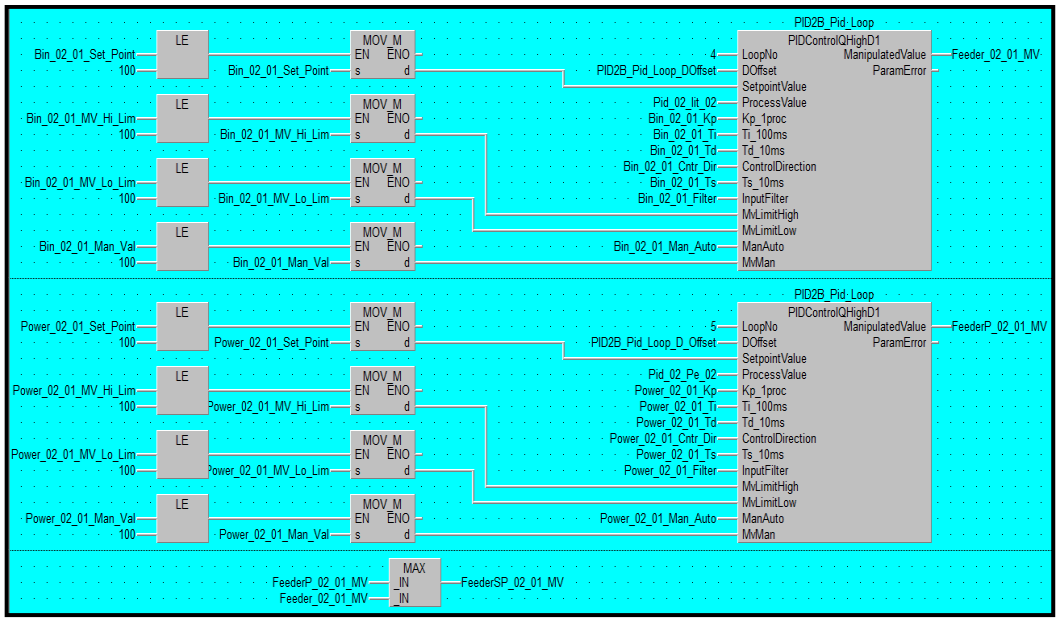

Figure 5.20 The PLC control model for crusher circuit optimization

The SCADA mimic was developed as depicted in Figure 5.21. The development attempted to match as much as possible the real plant at the Mowana mine with the addition of the proposed self-tuned controller, and feed hoppers interlocking the crusher feed conveyor.

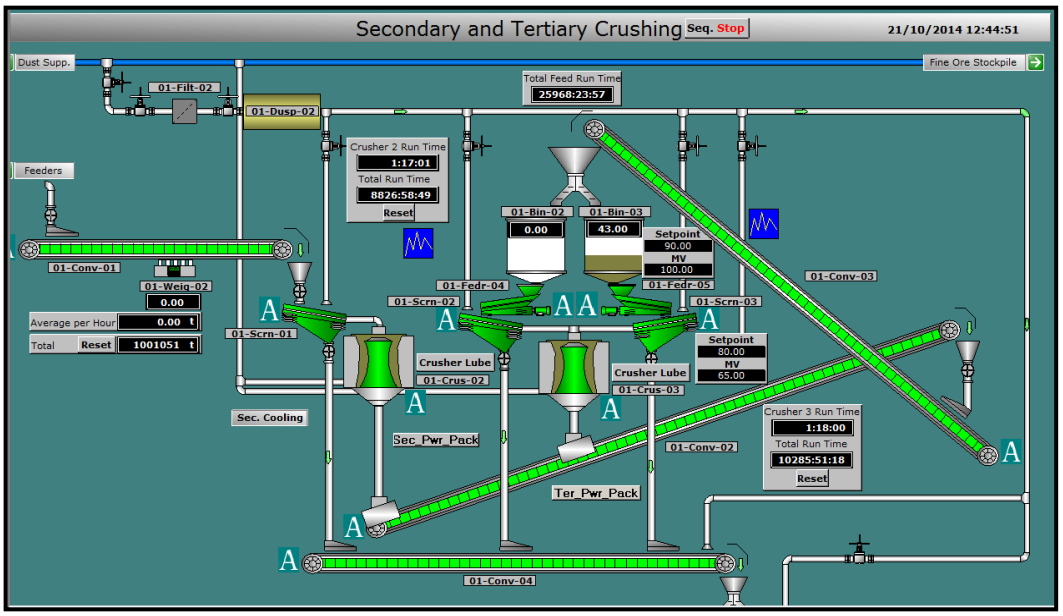

Figure 5.21 The simulator SCADA mimic

With the motor running on no-load, a power draw of 30 kW was observed. Upon in introduction of the step changes in set points from 30 kW to 50 kW and also from 50 kW to 70 kW, the power draw controller's response to disturbances occurring in the crusher was simulated.

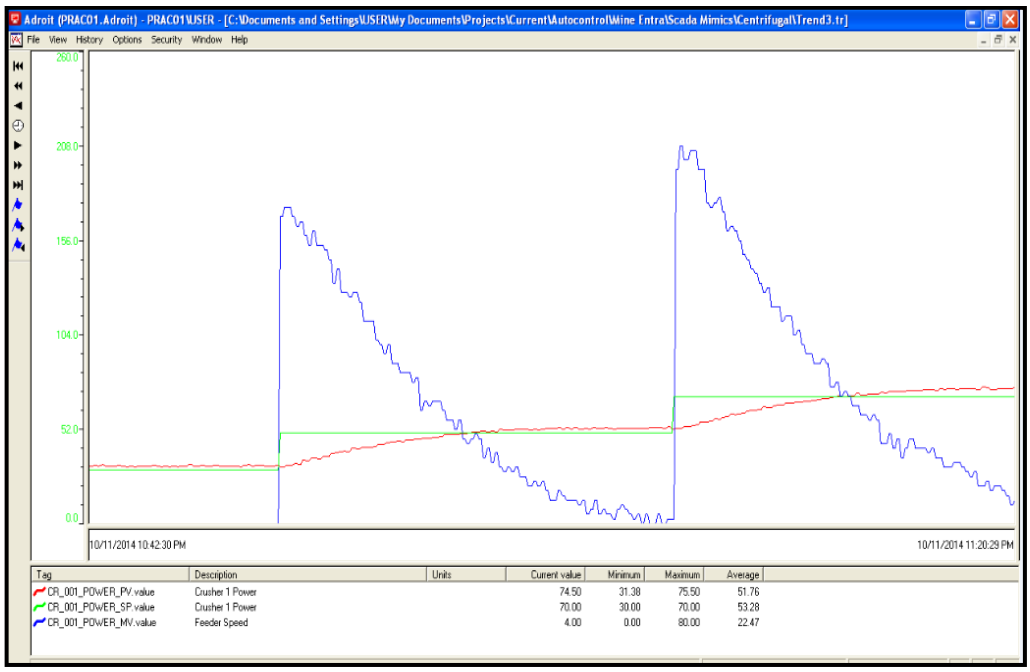

Figure 5.22 The simulated and optimised Adroit power draw response

The effects of disturbances on a power draw loop with feedback are presented in this simulation. From Figure 5.22, it can be seen that all the disturbances have similar dynamics. This observation is a consequence of plug flow pattern of the feed material and it results in a static relation between the input and output. Nevertheless, step-like interference would be feasible in reality. Feed rate is an exception because its dynamics hinges on the proportion between mass flow in and mass flow out.

It was also observed that the effect of feed material on crushing power is relatively small as compared to moisture and feed grading which are the only inputs that show recognizable variations in crushing power.

With the self-tuning design, the output to the pan feeder VSD reference will only be influenced by the controller with the greater output between

the two controllers. From the observation reported in Chapter 4, the crusher cavity level has a direct influence on the crusher motor power draw. Armed with this observation, it can be stated that during normal operation, the self-tuning controller would give approximately the same variable manipulation as demonstrated in Figure 5.22. That means the crusher can be run at optimum power draw and in choke feeding regime.

5.5 SUMMARISED FINDINGS

The crusher controllability can be assessed by contrasting the out-turn of worst-case integration of disturbances to the total result of controllable parameters. In the case of the simulations carried out for the Mowana crushing circuit, the controllable parameters cancel out the worst combination of the known potential disturbances. From a process control stand point this leads to a conclusion that the crushing process should be controllable for all reasonable production targets.

While it has been demonstrated that the crusher CSS is the most influential controllable parameter, it has also been demonstrated that crusher capacity and power can be used effectively to optimise the circuit. The use of crushing power and cavity level control is suitable for the crushing circuit since the crushers are running on a constant ES and the CSS is set and reset manually.

CHAPTER 6 CONCLUSIONS AND RECOMENDATIONS

In this research, the crushing circuit at Mowana mine has been identified as a bottleneck. The hypothesis was that the theoretical optimisation of the crushing circuit is attainable before any change implementation. The present chapter is a summary of the findings pertaining to the research undertaken. Answers to the questions initialized posed in the first chapter are presented. Recommendations for future work are also formulated.

6.1 Introduction

The main objective of this research was to formulate ways and means to formulate ways and means for opimising the operation of the Mowana crushing plant. To achieve the objectives of the objectives of the study, various methodologies were implemented and these are detailed in Chapter 3 to Chapter 5 of this research. Industrial scale and laboratory experiments were carried out to determine the parameters for the developed crushing circuit models.

A dynamic simulation model of the cone crusher at the Mowana mine was presented in this work. The dynamic model was developed for the purpose of designing a control system for the cone crusher. To this end, the crushing circuit was modelled by integration of steady state regression and transfer function models. The motivation for this approach was to capture the dynamics of the cone crusher as well as the flow of ore material. Transfer functions were used to model the crushing circuit dynamics while steady-state regression models were used to describe the static non-liniearities prevailing in the crushing process. Time constants were derived from calculations, experiments and theories.

In terms of analysis, two scenarios were considered: the effect of disturbances and the effect of controllable parameters. Controllable parameters are parameters that can be adjusted midst crusher operation in sequence to control and manipulate the crusher production. The simulated controllable parameters were CSS and ES and as for Mowana mine crushers these are semi-operational control parameters since they are only adjusted amidst shutdown or maintenance breaks. Disturbances are parameters which affect material flow in the crusher; namely, moisture, feed grading, crushability, feed rate, specific gravity and feed flakiness index. The simulated disturbances were feed size distribution (PSD), ore moisture (M), specific gravity (SG) and feed rate (Q).

Step functions were used in studying the effects of disturbances on the capacity and the power draw of the cone crusher. Although step-like disturbances are less likely to prevail in a real life set up, they provided good insights on the behavior of the simulation model at a design stage.

And in terms of prototyping, parameters of a PID controller were determined in the Simulink/MATLAB® environment. The simulation involved the optimisation of the control model as a function of the cavity level of and the power drawn by the cone crusher. A self-tuning control algorithm at PLC and SCADA level of control was then tested.

From a process control point of view crusher capacity and power draw have been proven in this research to be theoretically effective in the control and optimisation of the cone crusher circuit at Mowana mine. This was supported by the following summary of main findings.

6.2 Summarised findings

The outcome of the study presents an insight into the optimization of the Mowana mine crushing circuit through the design of a self-tuning controller for the cone crusher. The main findings from the dynamic simulations are:

- The present modus operandi at the Mowana mine is not optimal; and hence, is costly to run.
- The out-turn of each logical process disturbance can be cancelled by the use of a feedback control system.
- Additional investigations and full-scale tests on the real facility are necessary to confirm the findings

In order to assess whether the research objectives set out for this dissertation have been accomplished, the two research questions central to the work are commented upon below:

1. Can implementation of closed loop control systems in the process yield and improve production?

The process of crushing has an inherent number of feed material disturbances which the current implemented control modes at the Mowana mine crushing circuit have evidently failed to effectively compensate. In this research work, it has been shown that the influence of every reasonable process disturbance can be cancelled out by use of a feedback control system.

The simulations displayed that the effect of the controllable parameters surpass the domain of the resultant fluctuations in the crusher power draw and cavity level induced by rational process interference. This means if a state of art control techniques are implemented, the effects of all possible disturbances can be counteracted. Whilst it was demonstrated that the crusher CSS is without reservations the most influential controllable parameter, it was also shown that crusher capacity and power draw can be effectively utilised in optimising the crushing circuit.

The power draw controller PID parameters were determined by the Ziegler- Nichols tuning since it offers a tuning for disturbance rejection. The cone crusher controllability was evaluated by correlating the outcome of worst-case sequence of process material disturbances. Figure 5.22

shows distinctly that the optimised power draw and cavity level can be consistently realised if inhibiting circumstances like maximum power are not surmounted. Optimised power draw and cavity levels will result in significant increase in tons per hour crusher output at lower power draws.

2. Besides the commonly used parameter, CSS, in the adjustment of the product in cone crushers, is it possible to use other parameters for circuit optimisation?

Closed-side setting (*CSS*) emerged to be the most influential controllable parameter in comparison with the eccentric speed (*ES*). The effects of the *CSS* on the power draw and capacity of the cone crusher was much higher compared to that of the *ES*. On the same platform, it has been demonstrated that crusher capacity and power draw can be used effectively to optimise the circuit. In the case of the Mowana crushing circuit, the control of power and cavity level control was found to be a suitable strategy since the crushers are run on a constant *ES* while the *CSS* is set manually.

6.3 Recommendations for future work

From a process control point of view, crusher capacity and power draw have been proven theoretically to be effective in the control and optimisation of the cone crusher circuit at the Mowana mine.

The successive differentiation of optimisation outcome and measured data from the existing crushing circuit has in turn made it possible to assess the performances of the present crushing plant application. The analysis revealed that the crushing circuit under the current operating setup used at the Mowana mine is not optimal in terms of the studied parameters. A computer model was developed to simulate the operation and control of the Mowana mine crushing circuit. In extension to being an effective

teaching and training aid, the model can validate operational attributes of diverse design alterations and resolutions. Also, a study of the influence of disturbances on the process and the out-turn of feedback control has been well administered.

From this research work, it is recommended that:

- Full test of the self-tuning controller be implemented on the real facility for validation.
- Replacing the Mowana mine crusher under loaded motors with smaller standard or energy-efficient motors will improve efficiency.
- Additional investigations are required in order to validate the findings from this research.

The outcome of the simulations carried out in this research needs to be validated against the real Mowana crushing process control upgrade. This will then inform the modifications and recommended crusher motor resizing exercise to be implemented. After the modifications, the crushing circuit is to run until stability is attained. Whilst operating the cone crushing circuit at the same parameters, that is the same CSS and ES used before the changes, the plant performance is to be rated against the previous average tonnage per hour records. In comparison with the previously collected data, it should be evaluated if there was a significant increase in the crusher tonnage with the crusher running under choke conditions and lower power draws.

The projects department accepted the proposed self-tuning controller's full implementation on the crushing facility. Since this was classified as a project it has to go through the stages of approval up to the Mowana mine board of directors' level since it involves a control philosophy change. A control change document was approved and a project proposal was put in place with a plan of targeting plant annual shutdowns for implementation and commissioning.

It was further recommended that crushing plant operators be trained prior to the implementation of the suggested changes since the crushing circuit performance is dependent on their ability, experience and decision making. The simulator build in this program is to be used as a training platform. The absence of a laboratory cone crusher was a challenge in this research. It was also recommended that the simulator could be improved through the acquiring of a laboratory cone crusher.

REFERENCES

Asbjörnsson, G., 2013.*Modelling and simulation of dynamic behaviour in crushing plant.* Thesis for the degree of Licentiate of Engineering in Product and Production Development. Gothenburg: Chalmers University of Technology. p.15 – 36.

Balchen, J.G. and Mumme, K.I., 1988.*Process Control Structures and Applications*. New York: Von Nostrand Reinhold Co. Ltd .p. 16-21, 47 – 48.

Bond, F.C., 1952.The third theory of comminution. Trans AIME.193 (2).p.484 – 494.

Evertson, C.M., 2000.*Cone crusher performance*. PhD thesis in Product and Production Development. Gothenburg: Chalmers University of Technology. p. 1 – 49.

Gauldie, K., 1954. The output of gyratory crushers. Engineering. 30 (4).p.557 – 559

Gupta, A., Yan, D.S., 2006.*Mineral processing design and operations: An introduction*. Amsterdam : Amsterdam, Boston: Elsevier.p.129 – 141.

Herbst, J.A., et al., 2012. *The next step in mineral processing dynamic simulation to achieve the necessary standard for prefeasibility and feasibility studies – Modelling with discrete event maintenance combined with accurate continuous process modelling.* XXVI International Mineral Processing Congress. New Delhi: India

Hofler, A., 1990. *Fundamental breakage studies of mineral particles with an ultrafast load cell device.* PhD dissertation in the Department of Metallurgical Engineering. Salt Lake City, Utah: University of Utah

Hukki, R.T., 1975.*The Principles of Comminution: An Analytical Summary*. Engineering and Mining Journal. 170 (5).p.106-110

Hulthén, E., 2010.*Real-time optimization of cone crusher control with two variables*. Msc thesis in Product and Production Development. Gothenburg: Chalmers University of Technology.p.15 – 23.

Itävuo, P., 2009.*Dynamic modelling of rock crushing process*. Msc Thesis in a Degree Programme in Automation. Finland: University of Technology.p.102.

Itävuo, P., et al., 2011. Simulation and advanced control of transient behaviour in gyratory cone crushers. 8th International Mineral Processing Seminar (Procemin 2011), Santiago, Chile. p. 63 – 72

Khosrow, N., 2001. *Role of simulation software in design and operation of metallurgical pants: A case study*. Vancouver, British Columbia, Canada: AMEC Simons Mining and Metals.p.2 -9.

King, R.P., 2001. *Modelling and simulations of mineral processing systems*. Oxford, Great Britain: Butterworth-Heinemann.p.353 – 357.

Lee, E., 2012.*Optimization of Compressive Crushing*. PhD thesis in Product and Production Development. Gothenburg: Chalmers University of Technology.p.7 – 9.

Lindqvist, M., et al., 2006. *Influence of particle size on wear rate in compressive crushing.* Minerals Engineering. 19 (13). p. 1328-1335.

Mohammad, A.K.A., et al., 2011. *A design of a PID self-tuning controller using LabView*. A research in Mechatronics Engineering Department, Faculty of Engineering Technology. Amman, Jordan: Al-Balqa Applied University.p.161 – 171.

Nappier-Munn, T.J., et al., 1996.Mineral comminution circuits – Their operation and optimisation. Brisbane, Queensland: University of Queensland.p.66 - 99.

Nappier-Munn, T.J., et al., 1999. *Mineral Comminution Circuits-Their Operation and Optimisation.* Julius Kruttschnitt Mineral Research Centre, Queensland.

Sbarbaro, D., 2010. *Dynamic simulation and model-based control system design for comminution circuits.* In Sbarbaro, D. (ed): *Advanced Control and Supervision of Mineral Processing plants*. London: Springer. p. 213 – 245

Quist, J., 2012.*Cone crusher modelling and simulation*. MSc thesis in Product and Production Development. Gothenburg: Chalmers University of Technology.p.8 – 36.

Ruuskanen, J., 2006.*Influence of rock properties in compressive crusher performance*. PhD thesis. Finland: Tampere University of Technology.p.143 -193.

Truscott, S., 1923 .A Textbook of Ore Dressing. Macmillan & Co, London.p.44.

Walker, W.H., et al., 1937.Principles of chemical engineering.3rd Ed. Newyork: McGraw-Hill Book Company Inc.p.

Whiten, W.J., 1972.*The simulation of crushing plants with models developed using multiple spline regression*. Journal of the South African Institute of Mining and Metallurgy. xx(x). p. 257 – 264.

Whiten, W.J., 1984.*Model and control techniques for crushing plants.* In: *Control'84, Mineral/Metallurgical Processing*. Newyork: AIME. p. 217 – 225

Wills, B.A., 2006. Mineral *processing technology: an introduction to the practical aspects of ore treatment and mineral recovery*.6th Ed. London: Elsevier.p.108 – 115.

Airikka, P., 2012. *Continuous-time Parameter Identification using PI Controllers.* Tampere: Metso Corporation.p.1 – 2.

Andrew, L., et al., 2000. *Mineral Processing Pant: Design, Practice, and Control.* Littleton, Colorado, USA: SME.p.669 – 678.

Hulthén, E and Evertsson, C.M., 2009. *Algorithm for Dynamic Cone Crusher Control.* Minerals Engineering. 22(3). p. 296-303.

Evertson, C.M., 1999. *Modelling of Flow in Cone Crushers.* Minerals Engineering. 12 (12). p. 1479-1499.

Hulthén, E and Evertsson, C.M., 2011. *Real time Algorithm for Cone Crusher Control with two Variables*. Minerals Engineering. 24(9). p.987-994.

Karra, V.K., 1982. *A Process Performance Model for a Cone Crusher.* Proc. 14th Intern. Miner Process Congr. Toronto. p. 6.1-6.14.

Hulthén, E and Evertsson, C.M., 2008. *On Line Optimisation of Crushing Stage using Speed Regulation on Core Crushers.* XXIV International Mineral processing Congress. Beijing, China. p. 2396-2402.

Juhasz, A.Z. and Opoczky, L., 1990. *Mechanical Activation of minerals by Grinding Pulverizing and Morphology of Particles.* Budapest, Hungaray: Akademia Kindo-Ellis Horwood Ltd.

Giri, F. (ed)., 2010. *Block Oriented Non-linear System Identification.* Berlin Heidelberg: Springer. p. 293-312.

Appendix A

Figure A.1 Raw data of *CSS* measurements by the two analysts

CSS Measurements					
Samples	Measurement (mm)				
Run1_16_BN	16.08	16.06	16.04	16.05	16.06
Run1_16_TS	16.09	16.10	16.09	16.11	16.10
Run2_16_BN	16.22	16.21	16.21	16.19	16.19
Run2_16_TS	16.20	16.21	16.19	16.22	16.20
Run3_16_BN	15.78	15.82	15.80	15.83	15.77
Run3_16_TS	16.01	16.00	15.98	16.03	16.00
Run4_16_BN	17.13	17.10	17.08	17.10	17.09
Run4_16_TS	17.20	17.20	17.21	17.18	17.19
Run5_16_BN	16.03	16.04	16.07	16.05	16.06
Run5_16_TS	16.09	16.11	16.10	16.09	16.12

Figure A.2 Raw data for crusher feed particle size analysis

Crusher Feed		
Screen size (mm)	Mass Retained (g)	Passing Mass (g)
75.0	0	33665
53.0	12 316	21349
37.5	5 154	16195
26.5	2 911	13284
19.0	2 499	10785
16.0	1 168	9617
11.2	2 177	7440
8.0	1 452	5988
4.0	2 351	3637
-4.0	3 637	0
Total	33 665	
Belt speed:	2 m/s	
Distance:	1 m	
Throughput:	242 t/h	

Figure A.3 Raw data for crusher feed particle size analysis

Crusher Feed		
Screen size (mm)	Retained Mass (g)	Passing Mass(g)
75.0		46363
53.0	18 963	27400
37.5	4 249	23151
26.5	3 799	19352
19.0	2 236	17116
16.0	986	16130
11.2	1 908	14222
8.0	1 601	12621
4.0	3 372	9249
-4.0	9 249	0
Total	46 363	
Belt speed:	2 m/s	
Distance:	1 m	
Throughput:	334 t/h	

Figure A.4 Raw data for particle size distribution of the crusher product analysis

Crusher Product		
Screen size (mm)	Retained Mass (g)	Passing Mass (g)
75.0	0	40 003
53.0	0	40 003
37.5	0	40 003
26.5	0	40 003
19.0	132	39871
16.0	200	39671
11.2	4 901	34770
8.0	10 012	24758
4.0	10 762	13996
-4.0	13 996	0
Total	40 003	
Belt speed:	0.6 m/s	
Distance:	1 m	
Throughput:	86 t/h	

Figure A.5 Raw data for power draw as a function of cavity level experiment

Cavity Level (%)	Active power (kW)	Power factor (-)	V_{rms} (V)	I_{rms} (A)
0	79.87	0.65	532.3	52.2
	81.35	0.77	532.4	51.1
	80.15	0.74	531.9	50.5
	79.04	0.7	532.7	50.75
	80.1	0.68	532.2	52
25	90.27	0.65	531.1	128.5
	90.85	0.69	531.6	130.2
	91.35	0.78	532.9	129.1
	91.86	0.8	533.3	130
	91.07	0.68	534.1	131.2
50	129.65	0.7	532	188.9
	130.1	0.75	531.8	189.4
	128.2	0.75	531.7	189.1
	129.1	0.71	531.5	184.1
	131	0.73	531.9	186.4
75	160.94	0.62	529.8	215.8
	162.43	0.88	531	216
	161.32	0.69	530.1	216.9
	162.03	0.81	529.7	216.6
	162.18	0.85	531.4	216.7
100	209	0.78	529.4	275.6
	210.7	0.83	531.8	272.1
	208.4	0.79	531.4	273.1
	205.15	0.88	531.9	270.8
	212.1	0.77	531.7	277.4

Figure A.6 Raw data for power draw as a function of feed rate experiment

Feed rate (tph)	Active power (kW)	Power factor (-)	V_{rms} (V)	I_{rms} (A)
0	79.87	0.7	533.4	53.05
	81.35	0.71	531.8	52.98
	80.15	0.71	532.3	53.01
	79.04	0.7	532.8	53.02
	80.1	0.73	531.9	53.01
100	138.9	0.72	532	95.2
	138.7	0.73	531.9	95.18
	138.35	0.75	532.1	95.22
	138.2	0.74	532	95.23
	138.2	0.73	532.06	95.24
150	152.18	0.68	530.2	101.36
	154.2	0.83	531.4	102.05
	152.21	0.71	532.3	104.12
	153.68	0.81	530.9	103.53
	152.08	0.77	533.7	103.19
200	183.13	0.59	530.7	130.98
	183.11	0.67	531.6	131.27
	183.97	0.94	531.3	131.78
	184.95	0.85	530.9	131.93
	183.74	0.75	531	131.19
250	212.86	0.85	530.2	159.24
	214.55	0.69	530.9	158.87
	213.13	0.83	531.3	159.52
	214.28	0.79	531.9	158.12
	214.03	0.69	530.7	160.15
300	252.65	0.78	530.7	176.96

	252.68	0.77	530.6	176.99
	252.64	0.78	530.7	176.96
	252.67	0.78	530.8	176.94
	252.63	0.79	530.7	176.94
380	266.3	0.83	529.9	196.05
	265.8	0.8	530	198.3
	267.8	0.75	530.05	195.8
	264.8	0.82	530.1	197.4
	268.3	0.79	530.1	194.8

Appendix B

```
f = poly2sym([40.9, 9.2, 8.2, 4.8, 2.1]);
p = poly2sym([0, 0, 0, 0.3, 0.5]);
S = [1, 0, 0, 0,     0;
     0, 1, 0, 0,     0;
     0, 0, 1, 0,     0;
     0, 0, 0, 0.939, 0;
     0, 0, 0, 0,     0.779];
B = [0.022, 0,     0,     0,     0;
     0.099, 0.022, 0,     0,     0;
     0.194, 0.099, 0.022, 0,     0;
     0.156, 0.194, 0.099, 0.022, 0;
     0.237, 0.158, 0.194, 0.099, 0.022];
D = S*B;
E = S-D;
f-p
```

ans =

(409*x^4)/10 + (46*x^3)/5 + (41*x^2)/5 + (9*x)/2 + 8/5

```
% ------------------------------------------------
tspan = [0, 2];
y0 = 0;
mt = dsolve('Dm+0.565*m = (409*t^4)/10 + (46*t^3)/5 ...
+ (41*t^2)/5 + (9*t)/2 + 8/5','m(0) = 0');
t = [0:0.1:10];
y = (3822589160*t.^2)./1442897 ...
- 305599586495520./(18424351793*exp((113*t)/200)) ...
- (1527737056700*t)/163047361 ...
- (6336080*t.^3)/12769 + (8180*t.^4)/113 ...
+ 305599586495520/18424351793;
plot(t, y)
% ------------------------------------------------
```

```
mt = dsolve('Dm+1.242*m = (409*t^4)/10 + (46*t^3)/5 ...
+ (41*t^2)/5 + (9*t)/2 + 8/5','m(0) = 0');
y = (19548742700*t.^2)./79827687 ...
- 9724223597026600./(30784829042367 ...
*exp((621*t)/500)) ...
- (19369130404250*t)/49572993627 ...
- (38043400*t.^3)/385641 ...
+ (20450*t.^4)/621 + 9724223597026600/30784829042367;
hold on
plot(t, y)
% ------------------------------------------------
mt = dsolve('Dm+1.713*m = (409*t^4)/10 + (46*t^3)/5 ...
+ (41*t^2)/5 + (9*t)/2 + 8/5','m(0) = 0');
y = (155861008600*t.^2)./1675524699 ...
- 308774434149519200./(4916607735479931 ...
*exp((1713*t)/1000)) ...
- (304182156054500*t)/2870173809387 ...
- (147840400*t.^3)/2934369 + (40900*t.^4)/1713 ...
+ 308774434149519200/4916607735479931;
plot(t, y)
% ------------------------------------------------
mt = dsolve('Dm+2.198*m = (409*t^4)/10 + (46*t^3)/5 ...
+ (41*t^2)/5 + (9*t)/2 + 8/5','m(0) = 0');
y = (58718884100*t.^2)./1327373299 ...
- 29033173693105800./(1603202797905499 ...
*exp((1099*t)/500)) ...
- (55732294177250*t)/1458783255601 ...
- (35844600*t.^3)/1207801 + (20450*t.^4)/1099 ...
+ 29033173693105800/1603202797905499;
plot(t, y)
% ------------------------------------------------
mt = dsolve('Dm+2.445*m = (409*t^4)/10 + (46*t^3)/5 ...
+ (41*t^2)/5 + (9*t)/2 + 8/5','m(0) = 0');
```

```
y = (1259567480*t.^2)./38976723 ...
- 99848665875040./(9320152980483 ...
*exp((489*t)/200)) - (468747941300*t)/19059617547 ...
- (5644240*t.^3)/239121 + (8180*t.^4)/489 ...
+ 99848665875040/9320152980483;
plot(t, y)
hold off
% --------------------------------------------------
```